NOAA Technical Report NOS 71 NGS 6

Application of Digital Filtering to Satellite Geodesy

Rockville, Md.
May 1977

U.S. DEPARTMENT OF COMMERCE
National Oceanic and Atmospheric Administration
National Ocean Survey

NOAA TECHNICAL PUBLICATIONS

National Ocean Survey-National Geodetic Survey Subseries

The National Geodetic Survey (NGS) of the National Ocean Survey establishes and maintains the basic National horizontal and vertical networks of geodetic control and provides Government-wide leadership in the improvement of geodetic surveying methods and instrumentation, coordinates operations to assure network development, and provides specifications and criteria for survey operations by Federal, State, and other agencies.

The NGS engages in research and development for the improvement of knowledge of the figure of the Earth and its gravity field, and has the responsibility to procure geodetic data from all sources, to process these data, and to make them generally available to users through a central data base.

NOAA Technical Reports and Memorandums of the NOS NGS subseries facilitate rapid distribution of material that may be published formally elsewhere at a later date. A listing of these papers appears at the end of this publication. This publication is available from the National Technical Information Service, U. S. Department of Commerce, Sills Building, 5285 Port Royal Road, Springfield, Va. 22151. Price on request.

NOAA Technical Report NOS 71 NGS 6

Application of Digital Filtering to Satellite Geodesy

Clyde C. Goad

Geodetic Research and Development Laboratory
National Geodetic Survey

Rockville, Md.
May 1977

Doctoral Dissertation
School of Engineering and Architecture
Catholic University of America
Washington, D.C.

ACKNOWLEDGMENTS

ABSTRACT

Because the Earth is not a rigid homogeneous sphere, the path of a near-Earth satellite will deviate from a perfect ellipse. If accurate measurements of satellite orbits are available, one can hopefully deduce parameters from the observed orbital motions which model geophysical features. This dissertation gives the results and techniques to estimate one nonstationary variation in the Earth's gravity field--the principal lunar semi-diurnal (M_2) ocean tide.

Since the ocean tides cause periodic perturbations with periods greater than a week in the evolution of the Keplerian elements of a satellite, the mean Keplerian elements (osculating Keplerian elements less all short period oscillations) are studied. To date, no investigator has produced mean Keplerian elements accurate enough to observe the small variations caused by the M_2 ocean tides. To solve this problem, approximate analytical transformations have been applied which account for large first-order effects. Elimination of very high frequency effects is accomplished with the aid of an ideal low-pass filter. Precise transformations are only part of the solution, however. Accurate orbits significantly affected by ocean tides must be available. Fortunately, two such satellite orbits were obtained--1967-92A, a U. S. Navy satellite, and the NASA satellite, GEOS-3.

Two terms in the harmonic expansion of the M_2 global tide height can be observed. Estimates of these coefficients have been obtained. These estimates are somewhat smaller than recent published values obtained from numerical solutions of Laplace tidal equations.

Application of the satellite derived M_2 ocean tide coefficients to the problem of the deceleration of the lunar mean longitude yiels an estimate of -27.4 arc seconds/century^2 which is in close agreement with recent analyses of ancient eclipses and modern transit data. Because the entire tidal deceleration of the lunar mean longitude can be accounted for by the ocean tide model obtained in this study, it can be inferred that the solid tide phase lag must be less than 1°.

Knowledge of these important quantities in geophysics and space science, as well as the method developed to extract this information from satellite orbits, are considered important contributions of this study.

CONTENTS

LIST OF TABLES

LIST OF FIGURES

1. INTRODUCTION

The last twenty years of space exploration since the launch of Sputnik I in 1957 has revolutionized the science of geophysics. With the very first transmitted satellite data, it was possible to determine precisely the Earth's oblateness for the first time. Improvements in the knowledge of long wavelength features of the geopotential have been continuous. Today, geopotential spherical harmonic coefficients to degree and order (30, 30) are being estimated or improved. Atmospheric density studies obtained from satellite orbit analysis have also resulted in major improvements in man's knowledge of the structure of the atmosphere. By the late 1960's orbits of geodetic and navigation satellites were being analyzed at the meter level for such geodetic phenomena as polar motion and non-stationary variations in the Earth's gravity field. This dissertation gives the results and techniques used to estimate one such nonstationary variation in the Earth's gravity field—ocean tides from satellite orbit perturbations.

If the Earth were a rigid homogeneous sphere, satellite orbits due to this central force field would be perfect ellipses. However, the actual distribution of the Earth's mass is nonhomogeneous which gives rise to a rotating noncentral force field. Since the Earth is not a rigid body, tidal motion of the oceans and the deformation of the Earth's core and mantle create further complications. These phenomena plus the gravitational attraction of the other celestial bodies affect the satellite orbits and cause their paths to deviate from ellipses.

If accurate measurements of satellite orbits are available, one may hope to deduce these geophysical features from the observed orbital motions.

The problem investigated in this study is the deduction of the following

information from the observation of the orbits of 1967-92A and GEOS-3:

1. The M_2 tidal parameters which describe the semi-diurnal motion of
   the global ocean tide.

2. The rate of slowing down of the orbital motion of the Moon through
   the centuries because of resonance between the lunar motion and
   the motion of the M_2 ocean tide.

R. R. Newton (1965, 1968) and Kozai (1968) independently attempted

solutions from satellite ephemeris data for the parameters* which des-

cribe the solid Earth deformations due to the attraction of the Sun

and Moon. Since these nonstationary disturbances of the Earth's potential

perturb the orbits periodically with periods greater than a week, the

slowly varying features of satellite motion must be analyzed to recover

them. Newton pioneered a purely numerical technique for isolation of the

long-periodic effects of the Love numbers, while Kozai used traditional

analytic methods. Newton obtained a precision of 0.5 to 1.0 arc second

in the inclinations of his precessing Kepler ellipses. He rejected the

possibility of ocean tides corrupting his results since he considered

that it "contributed little to the total potential...The ocean tides

are rather random in phase and almost cancel when averaged over the

entire Earth at any particular instant." Kaula (1969) tried to explain

the large differences in Newton's results by a latitude dependence of

the solid Earth tide effect. Douglas et al. (1972, 1974) convincingly

showed an apparent latitude dependence by obtaining second degree Love

_____

* Love numbers named after A. E. H. Love.

numbers for GEOS-1 and GEOS-2 of 0.22 and 0.31, respectively. Lambeck
et al. (1974) clarified this entire subject when they showed that the
effects of the ocean tides were not at all random but were systematically
similar to the effects of the solid tide. The ocean tides are functions
of longitude and latitude and they were responsible for a large portion
of the difference between the GEOS-1 and GEOS-2 results.

Douglas et al. (1972, 1974) obtained improved mean elements by first
removing large perturbations in the elements due to low degree and order
terms of the geopotential before averaging. Since these parameters
reveal themselves as periodic variations in the elements, their removal
protects one against leaving behind residual effects due to averaging
over only a fraction of a period. The critical parameter which scientists
have tried to recover is the lag in the response of deformation of the
Earth to the attraction of the Sun and Moon. This lag is a very impor-
tant measure of the anelasticity of the Earth's core and mantle (Kaula,
1968). Because of the neglect of ocean tide effects, progress has been
limited in the estimation of the solid tide phase lag of the Earth from
satellite orbit analyses. Values ranging from 0° to 5° have been suggested
for the phase lag from tiltmeter observations and satellite orbit analyses.
Results of seismological data which yield information about rates of decay
of free oscillations of the Earth at periods of about 1 hour lead one to
believe that the lag should be between 0° and 1°.

Differencing common points of orbits determined from successive two-day
data spans have shown that conventional orbit determination results are
now accurate to a few meters (1 meter ≈ 0.03 arc second) along the direc-
tion of motion (along-track). If the along-track positions are known to
this accuracy, then the semi-major axes should be known to the centimeter

3

level. However, no one has yet demonstrated centimeter accuracies in their

mean elements. This inability to produce mean elements that have the same

accuracy as osculating elements was the initial impetus for this endeavor.

It was believed that if mean orbital elements could be obtained with a

precision of 0.01 arc second in the inclination or node (normally out-of-

plane components are known better than the along-track components), then

it would be possible to solve for meaningful ocean tide parameters. This

is advantageous since no modeling of the dynamics of the oceans would be

required. Lambeck et al. (1974) attempted a solution of the ocean tide

parameters affecting satellite orbits, but concluded that their results

were "not significant" because of the inadequate precision of the orbital

data.

Precise transformations are only part of the solution, however. Accu-

rate orbits significantly affected by ocean tides must be available.

Fortunately, two such satellite orbits were obtained — 1967-92A, a U. S.

Navy Navigation Satellite; and the NASA satellite, GEOS-3. Improved

transformations have been developed and the 1967-92A and GEOS-3 orbital

data have been analyzed. Even though only a few ocean tide parameters

can be obtained from satellite orbit perturbations, they have an extremely

important application to the tidal acceleration of the Moon.

In 1975 Lambeck applied the ocean tide theory developed in 1974 to the

problem of the orbital evolution of the Moon. Using the results of

numerical solutions to Laplace tidal equations, Lambeck obtained a

value of -35 arc seconds/century^2 for the lunar $\ddot{N}$ (acceleration of lunar

mean longitude) which seemed to agree well with observations of ancient

eclipses. Based on these results, Lambeck argued that since the predicted

4

value of $\dot{N}$ of the Moon from ocean tides matched the observed value of $\dot{N}$, then the effect of the solid tide was small. This supports the argument that the solid tide phase lag ($\dot{N}_{solid}$ is proportional to lag angle) must be close to zero. A subsequent analysis of ancient eclipse data (Muller 1974) and analysis of transits of Mercury (Morrison and Ward 1975) has shown the proper value of $\dot{N}_{moon}$ to be -26 to -28 arc seconds/century^2. Not only are the ocean tide results obtained in this study in reasonable agreement with numerical solutions of Laplace tidal equations, but they also yield a value of $\dot{N}_{moon}$, due to ocean tides, of -27.4 arc seconds/ century^2 — a value in close agreement with the recent results of Muller, and Morrison and Ward. This result is also supported by Kuo (1977) who estimates the solid tide phase lag to be less than 1.0^o based on data from a network of gravimeters placed along a parallel of latitude across the United States. A variation of 0.5^o in the solid tide phase lag causes the $\dot{N}$ results to change by no more than 1 arc second/century^2.

Knowledge of these important quantities in geophysics and space science, as well as the method developed to extract this information from satellite orbits, are considered important contributions of this study.

Chapter 2 reviews the equations derived by Kaula (1966) to eliminate the major perturbations due to the geopotential field, and discusses some of their physical interpretations. The advantage of using low-pass filtering before the averaging process is introduced, and several examples of ideal and actual mean element results are given.

The origin and representation of ocean tidal phenomena are discussed in detail in Chapter 3. The historic work of Doodson (1921) will be empha-sized as well as the recent efforts of Hendershott and Munk (1970), Lambeck

5

et al. (1974). The appropriate potential function in terms of Keplerian elements for ocean tide attractions is given and its long period characteristics are discussed.

The solid tide attraction is discussed in Chapter 4, and its corresponding potential is given. Expressions of this potential function in terms of the ecliptic Keplerian elements of the disturbing body (as opposed to Earth equatorial elements), which are derived in appendix I, are stated. The frequency equivalence between ocean tide and solid tide satellite perturbations are shown.

Chapter 5 discusses the data processing of the inclination and nodal perturbations of the two satellites 1967-92A and GEOS-3. Comparisons are made between observed orbit variations and predictions from numerical tide models, showing observational equations derived from each sequence of orbital elements. These observations are then reduced with a standard least-squares algorithm to yield estimates of the ocean tide parameters. These estimates, obtained entirely from satellite orbit perturbations, are then compared with current numerical solutions of Laplaces tidal equations.

The ocean tide results are applied to the lunar orbit evolution problem in Chapter 6. Comparisons are made between satellite ocean tide predictions of the lunar $\dot{N}$ and the observations of $\dot{N}$ from ancient eclipse and Mercury transit data.

2. GENERATION AND UTILIZATION OF MEAN KEPLERIAN ELEMENTS

2.1 Osculating Keplerian Elements

In order to observe the behavior of a history of a perturbed satellite ephemeris and compare this ephemeris with the theoretical history of an unperturbed one, an appropriate potential function must first be constructed and differential equations be drawn up in terms of suitable coordinates. By far the major cause of the deviation of motion of a near-Earth satellite from the theoretical path of two-body motion is the nonspherical geopotential field of the Earth. To be able to observe orbital variations of a few meters due to phenomena, such as tides, one must first remove the effects of the geopotential which range in magnitude up to tens of kilometers. In addition, the attractions of other disturbing celestial bodies must also be modeled, since their effects also can be many times larger than those geophysical parameters which, hopefully, will be recovered. One particular choice of coordinates which is well suited for such investigations is the set of osculating Keplerian elements. Osculating Keplerian elements are coordinates that instantaneously define the Kepler ellipse obtained from the satellite's position and velocity. Since the potential field is noncentral, these elements will continuously change. The Earth's attraction deviates only slightly from a central force field and, therefore, the osculating ellipse will retain most of the attributes of the Kepler ellipses. Also, use of the Keplerian elements is very beneficial because of the stable behavior of the out-of-plane elements (inclination and right ascension of the ascending node). Errors in energy (semi-major axis) will only affect the motion along the direction of motion (along-track). The symbols used

for these osculating elements throughout this report are as follows:

a — semi-major axis

e — eccentricity

i — inclination

Ω — right ascension of ascending node

ω — argument of perigee

M — mean anomaly

It will be seen that such forms of the potential would be rather expensive to use in integrating the orbit numerically on a computer, but they are very useful to use when analyzing the major amplitudes and frequencies which perturb the motion. The standard set of three second-order differential equations in terms of inertial Cartesian elements defining the motion can be transformed into a set of six first-order differential equations in terms of these new variables which is usually referred to as Lagrange planetary equations. The derivation can be found in many standard textbooks on celestial mechanics, such as Brown and Shook (1933) and Brouwer and Clemence (1961), and the results of this transformation are given here. For motion in a conservative force field, the differential equations of motion can be obtained from a scalar, normally called the potential. Let the potential function U be given as

$$U = \frac{\mu}{2a} + R \tag{2.1}$$

where $\frac{-\mu}{2a}$ is the total energy due to two-body attraction of the Earth and R represents all other effects, such as geopotential and third-body attractions. Then the set of six first-order equations is given by

$$\frac{da}{dt} = \frac{2}{Na} \frac{\partial R}{\partial M}$$

$$\frac{de}{dt} = \frac{1-e^2}{Na^2 e} \frac{\partial R}{\partial M} - \frac{(1-e^2)^{\frac{1}{2}}}{Na^2 e} \frac{\partial R}{\partial \omega}$$

$$\frac{di}{dt} = \frac{\cos i}{Na^2(1-e^2)^{\frac{1}{2}}\sin i} \frac{\partial R}{\partial \omega} - \frac{1}{Na^2(1-e^2)^{\frac{1}{2}}\sin i} \frac{\partial R}{\partial \omega}$$

$$\frac{d\Omega}{dt} = \frac{1}{Na^2(1-e^2)^{\frac{1}{2}}\sin i} \frac{\partial R}{\partial i}$$

(2.2)

$$\frac{d\omega}{dt} = \frac{- \cos i}{Na^2(1-e^2)^{\frac{1}{2}}\sin i} \frac{\partial R}{\partial i} + \frac{(1-e^2)^{\frac{1}{2}}}{Na^2 e} \frac{\partial R}{\partial e}$$

$$\frac{dM}{dt} = N - \frac{1-e^2}{Na^2 e} \frac{\partial R}{\partial e} - \frac{2}{Na} \frac{\partial R}{\partial a}$$

where $N = \sqrt{\mu/a^3}$,

μ is the gravitational constant G times mass of Earth. Nonconservative contributions must be included in (2.2) in terms of force components.

2.2 Keplerian Potential Function for Geopotential

Kaula (1961, 1966) has transformed the various potential functions into very useful forms as harmonic expansions in terms of the fundamental frequencies of the motion $\dot{\Omega}$, $\dot{\omega}$, $\dot{M}$. Let $V_{\ell m}$ stand for the degree ℓ and order m terms of the potential. Then

$$V = \sum_{\ell=2}^{\infty} \sum_{m=0}^{\ell} V_{\ell,m} = \sum_{\ell=2}^{\infty} \sum_{m=0}^{\ell} \frac{\mu a_e^{\ell}}{\ell+1} \sum_{p=0}^{\ell} F_{\ell mp}(i) \sum_{q=-\infty}^{\infty} G_{\ell pq}(e) S_{\ell mpq}(\omega,M,\Omega,\theta)$$

(2.3)

9

where
$$S_{\ell m p q} = \begin{bmatrix} C_{\ell m} \\ -S_{\ell m} \end{bmatrix} \begin{matrix} \ell\text{-m even} \\ \\ \ell\text{-m odd} \end{matrix} \cos\left[(\ell-2p)\omega+(\ell-2p+q)M+m(\Omega-\theta)\right]$$

$$+ \begin{bmatrix} S_{\ell m} \\ C_{\ell m} \end{bmatrix} \begin{matrix} \ell\text{-m even} \\ \\ \ell\text{-m odd} \end{matrix} \sin\left[(\ell-2p)\omega+(\ell-2p+q)M+m(\Omega-\theta)\right]$$

a_e is semi-major axis of the Earth,

θ is Greenwich sidereal angle

$C_{\ell m}$ and $S_{\ell m}$ are the standard cosinusoidal and sinusoidal coefficients when the potential is expressed in terms of spherical coordinates (latitude and longitude).

From (2.3) it is seen that summations over four subscripts must be performed to evaluate the total potential. It is for this reason that the potential function expressed as in (2.3) is not normally used when operationally integrating satellite ephemerides. For example, modeling to first order a typical geodetic satellite ephemeris to the sub-meter level could require more than 500 $\ell m p q$ sets.

The inclination functions $F_{\ell m p}(i)$ and eccentricity functions $G_{\ell p q}(e)$ are polynomials. The inclination polynomials are of finite degree, but the eccentricity polynomials are not. However, for small values of e (less than 0.2) the eccentricity polynomials do converge rapidly. A useful property to remember is that the leading term of $G_{\ell p q}(e)$ is proportional to $e^{|q|}$, where e is eccentricity. Therefore, the summation over q is usually restricted to only small values of $|q|$ depending on

the precision required.

2.3 Secular, Resonant, m-Daily, and Long Period Contributions

Notice the convenience of form (2.3). After substituting (2.3) into (2.2), it is easy to see how the element perturbations are driven by a linear combination of the three fundamental frequencies $\dot{\omega}$, $\dot{M}$, $\dot{\Omega}-\dot{\theta}$. For example, $\dfrac{d\Omega}{dt}$ is given by

$$\frac{d\Omega_{\ell mpq}}{dt} = \frac{\mu a_e^{\ell}}{a^{\ell+1}} \frac{\partial F_{\ell mp}(i)}{\partial i} G_{\ell pq}(e) \, S_{\ell mpq}(\omega, M, \Omega, \theta)$$

$$S_{\ell mpq} = \begin{bmatrix} C_{\ell m} \\ S_{\ell m} \end{bmatrix} \begin{matrix} \ell-m \text{ even} \\ \cos \gamma \\ \ell-m \text{ odd} \end{matrix} + \begin{bmatrix} S_{\ell m} \\ C_{\ell m} \end{bmatrix} \begin{matrix} \ell-m \text{ even} \\ \sin \gamma \\ \ell-m \text{ odd} \end{matrix}$$

$$\gamma = (\ell-2p)\omega + (\ell-2p+q)M + m(\Omega-\theta)$$

If $\ell-2p = \ell-2p+q = m = 0$, the angular argument is identically zero; and such ℓmpq combinations would give secular terms ($\dot{\Omega}_{\ell mpq}$ = const).

If $\ell-2p+q = 0$ and $m \neq 0$, then the derivative would go through m cycles in a day. Such an ℓmpq combination is called an m-daily term. If $\ell-2p+q = m = 0$, then both the mean anomaly rate and the rotation rate of the Earth are not present. Thus, the only angular element which is present is the argument of perigee which is very slowly changing. Any term containing only ω is called a long period term. Resonance occurs when the orbital motion and the rotation of the Earth beat against one another. This happens when

$$(\ell-2p+q)\dot{M} + (\ell-2p)\dot{\omega} \approx m(\dot{\theta}-\dot{\Omega}) \qquad\qquad \ell-2p+q \neq 0$$

is satisfied. As the equality becomes more exact, the resonance period can become quite long.

2.4 Analytical Approximations and Mean Keplerian Elements

As will be shown in Chapter 3, perturbations due to certain phenomena, such as tides, can only be detected when long period effects are studied. This is accomplished by converting from osculating Keplerian elements to a set of elements with as many of the short period effects removed as possible. That is, the history of any osculating element $a_i(t)$ $(i=1,2...,6)$ can be expressed as the sum of long and short periodic contributions

$$a_i(t) = \bar{a}_i(t) + \Delta a_i(t)$$

where $\bar{a}_i(t)$ is the sum of the low frequency, constant, and secular contributions, $\Delta a_i(t)$ represents the high frequency oscillations. The $\bar{a}_i$ are called mean Keplerian elements. The first step in the process of converting from osculating to mean variables is to remove all terms that have M and θ as angular arguments, which is equivalent to removal of short period terms.

First-order approximations to the perturbations are found by assuming that $a, e, i, \dot{M}, \dot{\omega}, \dot{\Omega}$ are constant. This results in an equation of the form

$$\dot{x}(t) = K_1 \sin(\alpha_0 + \dot{\alpha}t) + K_2 \cos(\alpha_0 + \dot{\alpha}t)$$

where K_1, K_2, α_0, $\dot{\alpha}$ are constants.
The above can be integrated to give

$$x(t) = -K_1 \cos(\alpha_0 + \dot{\alpha}t) + K_2 \sin(\alpha_0 + \dot{\alpha}t).$$

When $|\dot{\alpha}|$ is small, as is the case of resonance, then the perturbations can become very large. Excluding this case, substitutions of $V_{\ell mpq}$ into Lagrange planetary equations and integrating as above yields the perturbation equations as given by Kaula (1966):

$$\Delta a_{\ell mpq} = \mu a_e^\ell \frac{2F_{\ell mp} G_{\ell pq} (\ell-2p+q) S_{\ell mpq}(\delta)}{Na^{\ell+2}} \cdot \frac{1}{\dot{\delta}}$$

$$\Delta e_{\ell mpq} = \mu a_e^\ell \frac{F_{\ell mp} G_{\ell pq} (1-e^2)^{\frac{1}{2}}[(1-e^2)^{\frac{1}{2}}(\ell-2p+q)-(\ell-2p)]S_{\ell mpq}(\delta)}{Na^{\ell+3}} \cdot \frac{1}{\dot{\delta}}$$

$$\Delta i_{\ell mpq} = \mu a_e^\ell \frac{F_{\ell mp} G_{\ell pq} [(\ell-2p)\cos i - m]S_{\ell mpq}(\delta)}{Na^{\ell+3}(1-e^2)^{\frac{1}{2}} \sin i \; \dot{\delta}}$$

$$\Delta \Omega_{\ell mpq} = \mu a_e^\ell \frac{(\partial F_{\ell mp}/\partial i) G_{\ell pq} \overline{S}_{\ell mpq}(\delta)}{Na^{\ell+3}(1-e^2)^{\frac{1}{2}}\sin i \; \dot{\delta}} \qquad (2.4)$$

$$\Delta \omega_{\ell mpq} = \mu a_e^\ell \frac{[(1-e^2)^{\frac{1}{2}}e^{-1}F_{\ell mp}(\partial G_{\ell pq}/\partial e)-\cot i(1-e^2)^{-\frac{1}{2}}\partial F_{\ell mp}/\partial i)G_{\ell pq}]\overline{S}_{\ell mpq}(\delta)}{Na^{\ell+3}e\dot{\delta}}$$

$$\Delta M_{\ell mpq} = \mu a_e^\ell \frac{[-(1-e^2)e^{-1}(\partial G_{\ell pq}/\partial e) + 2(\ell+1)G_{\ell pq}]F_{\ell mp}\overline{S}_{\ell mpq}(\delta)}{Na^{\ell+3} \; \dot{\delta}}$$

$$- \frac{3\mu a_e^\ell F_{\ell mp} G_{\ell pq} \overline{S}_{\ell mpq}(\delta) (\ell-2p+q)}{Na^{\ell+3} \; \dot{\delta}^2}$$

where $N = \sqrt{\mu/a^3}$ $\qquad\qquad$ $\delta = (\ell-2p+q)M + (\ell-2p)\omega + m(\Omega-\theta)$,

$\overline{S}_{\ell mpq}$ is the integral of $S_{\ell mpq}$ with respect to its argument.

Since C_{20} is approximately 1000 times greater than any other geopotential coefficient, the C_{20} secular terms very closely resemble the actual secular rates of the elements Ω, ω, M

$$\dot{\Omega}_{ref} = \frac{3N\ C_{20}a_e^2}{2a^2(1-e^2)^2}\ \cos\ i$$

$$\dot{\omega}_{ref} = \frac{3N\ C_{20}a_e^2}{4a^2(1-e^2)^2}\ (1 - 5\ \cos^2 i\ ) \tag{2.5}$$

$$\dot{M}_{ref} = N - \frac{3N\ C_{20}a_e^2}{4a^2(1-e^2)^{3/2}}\ (3\ \cos^2 i - 1)$$

These angular rates are used as the reference angular rates in the denominators of equation (2.4), i.e., it represents deviations about a secularly precessing Kepler ellipse $(a, e, i, \dot{\Omega}, \dot{\omega}, \dot{M}$ constants).

Recalling that long period perturbations (excluding resonance) due to the geopotential occur when only ω appears in the angular argument, extremely long periods will occur when $\omega \approx 0$. From the above $\dot{\omega}_{ref}$ equation, it is found that $\dot{\omega} \approx 0$ when

$$\cos\ i = \pm\ \frac{\sqrt{5}}{5}\ \text{or}\ i = 63.4^o,\ 116.6^o$$

This situation is usually referred to as the "critical inclination" problem.

Polar orbiting satellites ($i = 90^o$) exhibit no node motion due to C_{20}. Satellites with inclinations less then 90° have node regressions ($C_{20} < 0$), while satellites with retrograde orbits ($i > 90^o$) exhibit progressions of the node.

14

Expressions for the first-order perturbations due to third-body attrac-
tions are given by Kaula (1961) and are similar to (2.4). Such expres-
sions will be discussed in Chapter 4 when the effects of solid-body tides
are analyzed.

2.5 Previous Numerical Transformation Methods

Transforming from osculating to mean elements or, in other words,
completely eliminating all short period terms could be performed entirely
using analytical techniques. However, if a transformation is required
to remove all short-period terms to the centimeter level, one must con-
sider second-and higher-order terms in addition to a vast number of
first-order perturbations. To eliminate the complexity and large amounts
of computer time required to perform such transformations, R. R. Newton
(1965) fitted a secularly precessing Kepler ellipse to a closely-spaced
ephemeris of Cartesian elements. He obtained a precision of 0.5 to 1.0
arc second in the mean inclination of U. S. Navy navigation satellites.
He then used these "mean" Keplerian elements to recover lumped values of
the solid Earth tidal Love numbers and phases. There were large varia-
tions in his results which Lambeck et al. (1974) properly explained as
the neglect of the influence of ocean tides.

Douglas et al. (1972) modified this procedure by removing large first-
order perturbations from a sequence of closely-spaced osculating
Keplerian elements prior to the least squares fit to a secularly pre-
cessing ellipse. They obtained a fit of 0.1 arc second in the mean
inclinations and 10 cm in the mean semi-major axes of the GEOS-1 and
GEOS-2 satellites.

Also unaware of the systematic effects of ocean tides on orbits of near-Earth satellites, Douglas et al. (1972) using this improved method of obtaining mean elements obtained very precise and differing values of the solid tide Love number k_2 from the two satellites, which implied a latitude dependence on the particular orbit being analyzed.

It was the results of Douglas et al. (1972) that led to the present effort to try to produce mean Keplerian elements having a precision of 0.01 arc second in mean inclination and 1 cm in the mean semi-major axis (1 cm change in the mean semi-major axis would cause the position in the direction of the velocity vector to change by only 1 m in a day). To obtain their results, Douglas et al. corrected the osculating elements for geopotential terms through degree and order (4,4) before averaging over a one-or two-day sequence to extract the single set of mean elements.

2.6 Application of Low-Pass Filtering

It was felt that the use of Kaula's harmonic approach should be extended to include all significant perturbations due to the geopotential through degree and order (30,30). Table 1 gives a few selected effects on the semi-major axis and inclination of GEOS-2. It is easily seen that even for this small collection of frequencies, one time span over which all listed terms have an integer number of periods would be extremely long. The cost of integrating such a lengthy trajectory would be prohibitive. One solution to this problem is the use of a low-pass filter to numerically remove high-frequency effects. This is a natural extension of the averaging process used by Newton and Douglas et al.

16

Table 1.—Selected geopotential perturbations on GEOS-2, GEM 6 gravity model

Degree	Order	Frequency (Cycles/Day)	Δa (m)	Δi (sec)
2	0	25.6	8000.	15.
		12.8	130.	0.5
		76.9	0.3	.0002
2	2	23.6	8.	.14
		1.998	0	4.7
		27.6	21.	.2
3	1	1.003	0.	.05
		37.4	12.	.1
		11.8	8.	.1
13	13	0.18	2.6	.5
14	13	.17	.2	.04
		.16	.4	.07

First, the number of ℓmpq sets required to achieve centimeter precision would be diminished. That is, only perturbations with amplitudes larger than 1 m, with periods shorter than the chosen cutoff frequency, must be removed since the filter will "catch" or effectively throw out all perturbations with frequencies greater than the cutoff frequency. However, all significant variations with periods greater than the cutoff period must still be modeled. Thus, the filter would tend to keep down the number of ℓmpq sets and at the same time eliminate all high frequency effects of all orders. The reference to higher-order effects is analogous to higher-order terms in a Taylor series expansion. To evaluate the first-order approximations, $a,e,i,\dot{\Omega},\dot{\omega},\dot{M}$ were assumed to be constant when, in fact, they were not. For example, the predicted variation in the semi-major axis, due to the twice per revolution effect of C_{20}, is in the neighborhood of 8 km. This approximation is good to about 20 m which can be accounted for if higher-order terms are considered.

Low-pass filtering can be described simply as multiplying any signal in frequency space by a unit step function which is equal to zero above any chosen cutoff frequency. This is expressed mathematically by

$$\bar{A}\,(\omega) = A\,(\omega) \cdot H\,(\omega)$$

where $\bar{A}\,(\omega)$ is Fourier transform of filtered signal

$A\,(\omega)$ is Fourier transform of input signal $\qquad$ (2.6)

$$H\,(\omega) = \begin{cases} 1 & |\omega| < \omega_c \\ 0 & |\omega| \geq \omega_c \end{cases}$$

Since multiplication in frequency space can be expressed as a convolution in the time domain, equation (2.6) can be written equivalently as

$$\bar{a}(t) = \int_{-\infty}^{\infty} a(\tau) \, h(t-\tau) \, d\tau$$

where $\bar{a}(t)$ is filtered signal   (2.7)

$a(t)$ is input signal

$$h(t) = \frac{\sin(\omega_c t)}{\pi t}$$

A computer implementation of equation (2.7) has been programmed using the well known Simpson-rule algorithm. Two shortcomings of the above procedure must be pointed out. First, the limits of integration $(-\infty, \infty)$ must be replaced with realistic finite limits $(0, T)$. For all results quoted here, a value of T equal to two days was used. To avoid transient effects near the endpoints caused by the integration over a finite interval, only filtered values during the middle day were actually used in the averaging process. Second, even though an extremely small cutoff frequency is preferred, one is limited by the duration of the finite span of data to be filtered. Eight-cycles per day was chosen for the results here.

The advantage of the filter can be easily seen by comparing figures 1 and 2. Figure 1 contains the semi-major axis of GEOS-2, after first-order corrections, using only the GEM-6 geopotential model (Lerch et al. 1974) in the satellite equations of motion. Notice the scale required to display these elements is at the 20 m level, the expected second-order effect due to J_2. The high frequency of the residual effects is also pronounced.

19
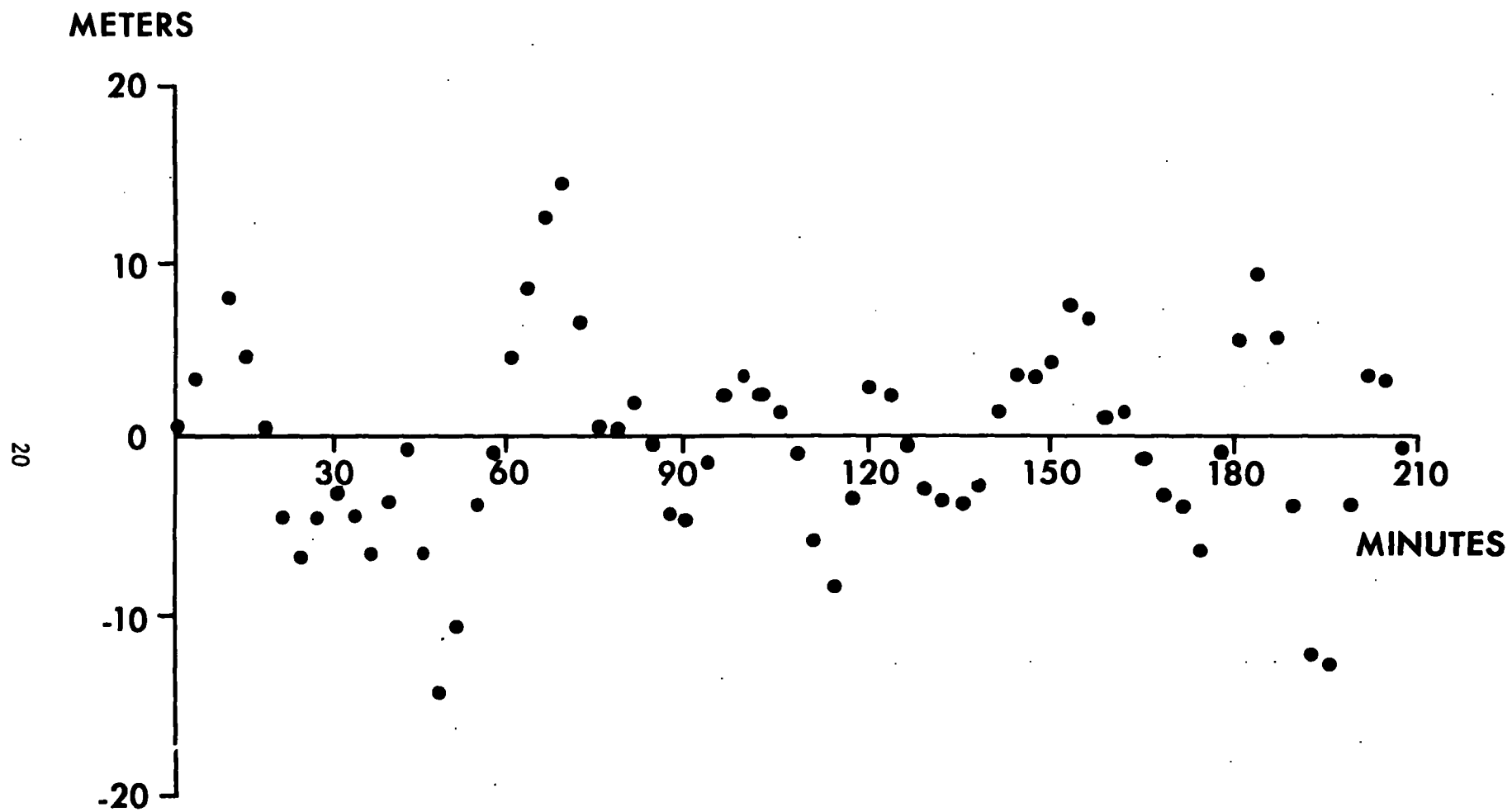
Figure 1.--Semi-major axis after first-order correction.

Figure 2 shows the same GEOS-2 elements used in figure 1 after passing them through the low-pass filter described above. The scatter about the average value is reduced to an rms of 3 cm, and the high frequency signature has been eliminated.

Figure 3 contains the unfiltered and filtered values of the inclinations less first-order corrections. The dominant slope is due to long-period variations which should be present in all terms except the semi-major axis. The scatter in the filtered inclinations is less than 0.02 arc second, which is less than the level expected of such phenomenon as the M_2 tidal effect, while the scatter of the unfiltered points is about 0.1 arc second.

Figure 4 gives a seven-day history at daily intervals of the filtered and unfiltered semi-major axes after averaging over a day. The scatter of the unfiltered mean elements is of the order 5 cm, while the filtered points are smooth to the precision of the graph and have a definite frequency content equal to the beat period of the 13th order resonances. This effect is believed to be a second-order interaction of J_2 with the resonant terms. The comparison leads one to believe that at least 5 cm of the 10-cm scatter experienced by Douglas et al. (1972) could have been due to inaccuracies in the transformations.

Figure 5 shows the history in the filtered mean semi-major axis of GEOS-2 during two weeks in June 1968. The elements were obtained from two-day arcs of optical flash data. The apparent sinusoidal variation with a period of approximately six days is due to unaccounted-for resonant effects, and the secular decay is due to the combination of drag and solar radiation pressure effects. Note that the random component of the signal shown in figure 5 is at the centimeter level. Numerous
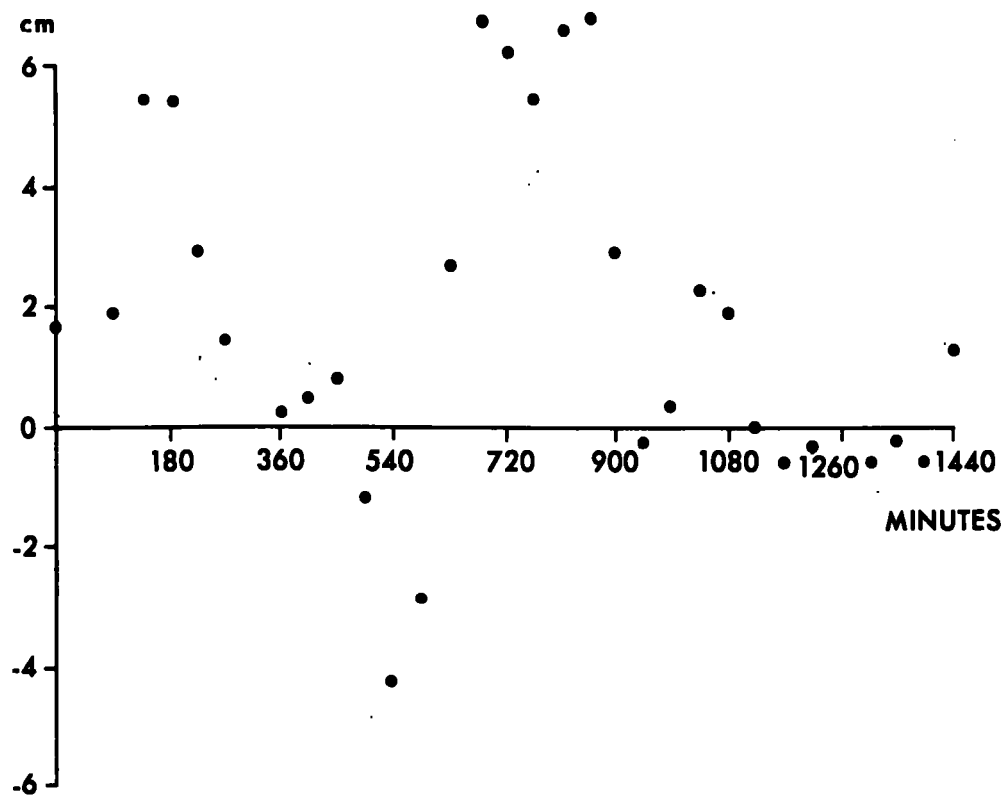
Figure 2.--Semi-major Axis After Filtering
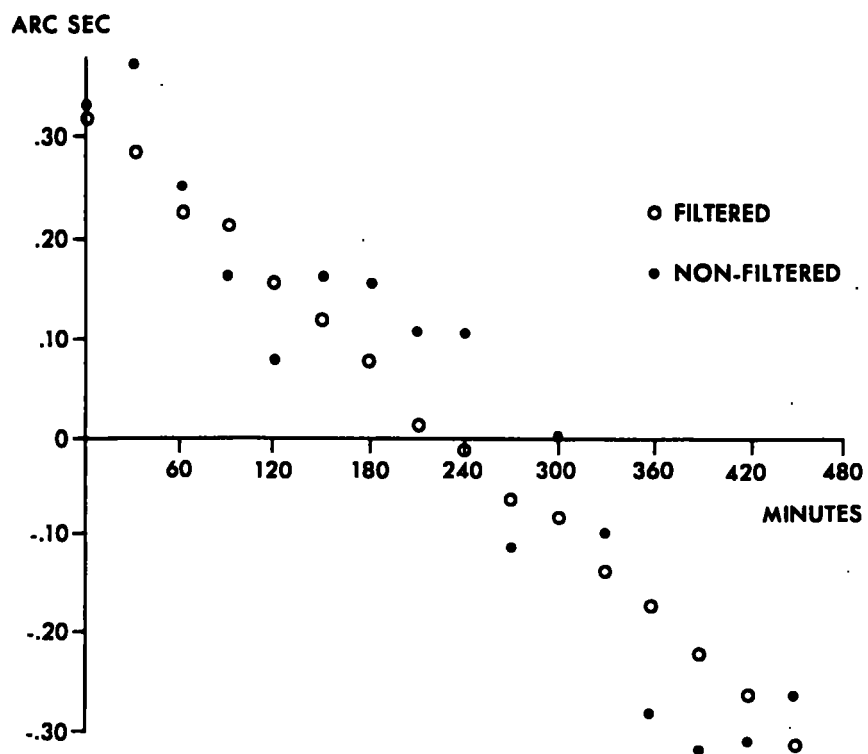
Figure 3.--Filtered versus Nonfiltered Inclinations
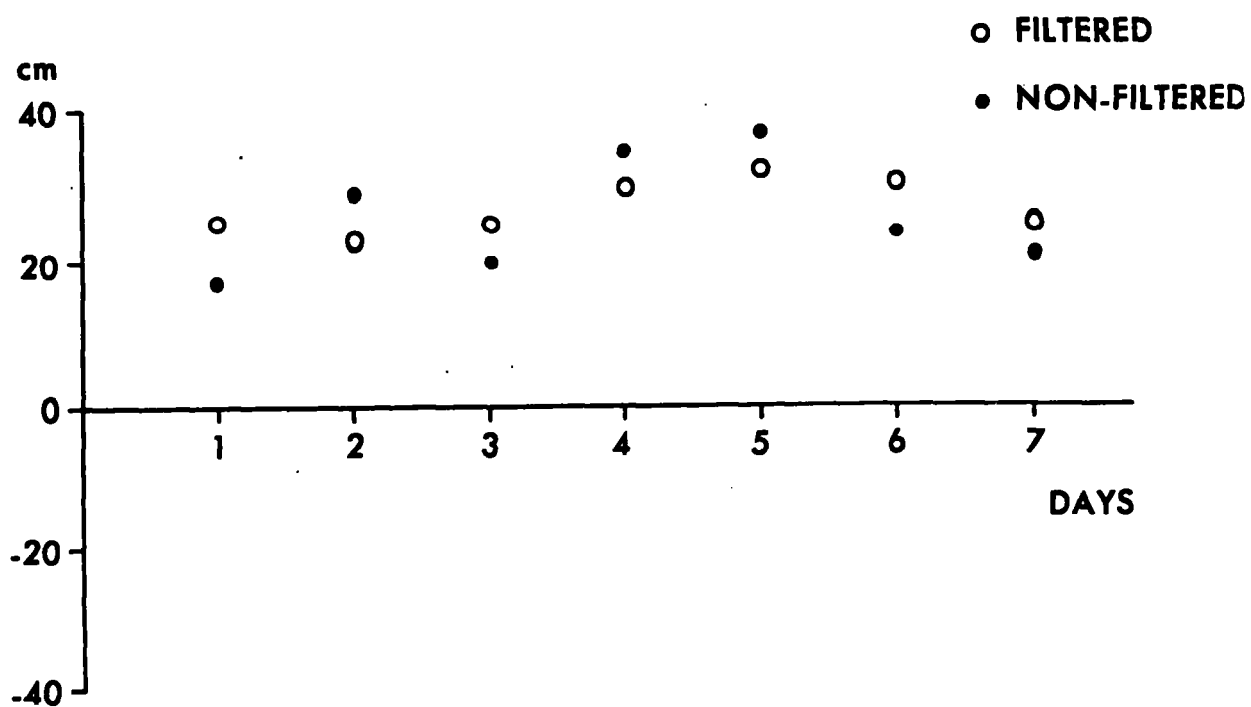
Figure 4.—Daily Mean Semi-major Axes from a 7-Day Ephemeris
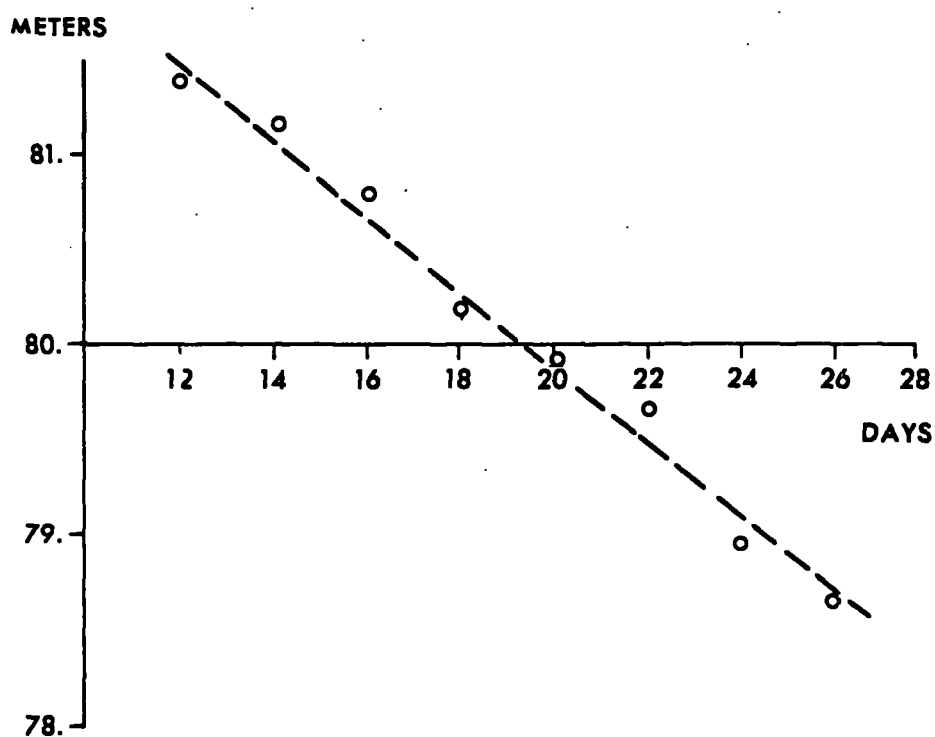
Figure 5.—Mean Filtered GEOS-2 Semi-major Axes From
Optical Flash Data—GEM 1 Revised.

applications of this technique exist not only to determine geodetic and geodynamic parameters, but also to evaluate the most subtle radiation and atmospheric effects.

2.7 Damping Effect of Averaging

Equally important in the conversion from osculating to mean elements is the removal of the direct lunar perturbations prior to averaging. The direct lunar perturbation corresponding to the semidiurnal M_2 frequency on the mean inclination has an amplitude 50 times greater than the ocean tide effect, so that any damping of the direct effect due to averaging will cause large errors in the ocean tide parameter determination. It is easy to show that a sinusoidal variation of frequency ω averaged over an interval 2Δ has its phase unchanged and its amplitude damped by a factor $\sin(\omega\Delta)/\omega\Delta$. As will be shown in Chapter 3, the dominant effect of the semi-diurnal M_2 tide is a semi-monthly orbit perturbation. With a one day average this damping amounts to about 1% and thus would produce an error of 50% in the ocean tide signal if allowed to occur.

2.8 Tidal Perturbations from a Sequence of Mean Elements

To isolate those perturbations due to tides and other geophysical parameters of interest, one must first pass the sequence of mean elements through an orbit determination program which properly models as many of the terms of the differential equation that are not to be estimated or improved. Fortunately, such a program was available from NASA Goddard Space Flight Center, Greenbelt, Maryland, This computer program, implemented by Williamson and Mullins (1973), is called ROAD (Rapid Orbit Analysis

24

and Determination). The force model used in ROAD is based on Kaula's work. Only long period, secular, and resonant terms are used which allows the numerical integrator to use stepsizes of a revolution or longer, as compared to conventional orbital integrators which normally use 1/75 to 1/100 revolution stepsizes. Such a program is very useful when analyzing long sequences of mean elements and predicting satellite life times (Wagner and Douglas, 1970). The possible force model parameters available to the ROAD user are the following:

- up to 200 ℓmpq sets - any degree and order term can be used to (40,40)
- solar and lunar third-body attractions.
- solar radiation pressure
- atmospheric drag
- solid tides
- dynamic effect of precession and nutation
- second order J_2 secular effects

All the above options were exercised when analyzing the data for this study. The application of the third-body effects of the Moon and Sun was especially useful. As will be shown in Chapter 3 and Chapter 4, the solid and ocean tides have the same frequency spectrum as do the direct effects of the disturbing bodies. Thus, ROAD was used quite effectively to eliminate or filter out the direct effects of the Sun and Moon so that only perturbations due to solid and ocean tides would remain when the ROAD theoretical orbit was subtracted from the actual satellite mean element ephemeris.

2.9 Aliasing

One might think that fitting an orbit to the mean element data could cause the fitted orbit to adjust to alias the parameters sought, e.g., as the ocean tides. Such aliasing should not happen in this case, however. The orbit is predominately governed by the central body and J_2 attractions. Thus, the orbit determination must first satisfy these dynamical constraints before any other much smaller terms in the potential function can be considered. That is, effects such as zonal and tesseral harmonics and solid and ocean tides are driven by the massive effects of central body and oblateness effects. This will be made even more evident when analytical approximations to tidal perturbations are obtained.

3. OCEAN TIDES

3.1 Background

The ebb and flow of the ocean tides on the shore have always fascinated and stimulated mankind. As pointed out by E. P. Clancy (1968), an ancient Roman author, Pliny, was aware of the dependence of tides on the motions of heavenly bodies as early as the first century A.D. From Pliny's Historia Naturalis we find the following: "Much has been said about the nature of waters; but the most wonderful circumstance is the alternate flowing and ebbing of the tides, which exist, indeed, under various forms, but is caused by the Sun and the Moon. The tide flows and ebbs twice between each two risings of the Moon, always in the space of twenty-four hours. First, the Moon rising with the stars swells out the tide, and after some time, having gained the summit of the heavens, she declines from the meridian and sets, and the tide subsides. Again, after she has set, and moves the heavens under the Earth, as she approaches the meridian on the opposite side, the tide flows in; after which it recedes until she again rises to us. But the tide the next day is never at the same time with that of the preceding."

Of course Pliny was referring to the principal lunar semi-diurnal frequency which Darwin (1898) gave the name M_2 (M for Moon, 2 for twice per day) and which has a period of 12.42 hours.

Even though the correlation of tides to the motion of the Sun and Moon were known to ancient observers, it was not until 1687 that Sir Isaac Newton in his Principia was able to construct a simple mathematical model for tidal phenomena. Based on his law of gravitation, Newton predicted the occurrence of spring and neap tides, diurnal and elliptic inequalities.

27

Laplace in 1773 was the first to formulate the differential equations of motion (which now are usually referred to as Laplace tidal equations). In his _Mécanique céleste_, Laplace solved the idealized case of a fluid covering the entire Earth under the influence of forced oscillations.

The obvious rise and fall of tides caused man to leave records of the ebb and flow as well as tidal crests along coasts and estuaries. In 1866 Lord Kelvin made the first harmonic analysis of such tidal observations. This procedure was quickly adopted. In 1898 George Darwin, in his book _The Tides_, provided a detailed description of the tide generating potential and associated frequencies. This work was the authoritative reference for approximately 25 years.

In 1921 A. T. Doodson, recognizing the fact that Darwin's work was based on variations in equatorial angular arguments of the Sun and Moon, revised Darwin's theory to represent the tide raising potential in terms of the ecliptical rather than equatorial variables.

The angular arguments of Doodson's trigometric series and their periods are given in table 2. The lunar mean longitude is the sum of the lunar node, mean anomaly, and perigee angles. The node is referred to the ecliptic. The mean longitude of the lunar perigee is the sum of the node and perigee angles which are again measured in the ecliptic. Likewise, the solar mean longitude is the sum of the perigee and mean anomaly angles. Thus, each of the fundamental angular quantities of both the Sun and Moon can be broken down into linear combinations of their mean Keplerian angular values. In addition, evaluation of local mean lunar time will require information about the Earth's rotation.

Table 2.—Six fundamental angular arguments of
the Earth-Moon-Sun system

Representation			
This study	Doodson	Description	Period
β_1	τ	mean lunar time reduced to an angle $\tau = \theta_G - s$ where θ_g is the longitude of Greenwich	12.42 hr
β_2	s	Moon's mean longitude	27.3215 d
β_3	h	Sun's mean longitude	365.2422 d
β_4	p	longitude of Moon's perigee	8.847 yr
β_5	$N' = -N$	N is the longitude of the Moon's ascending node	18.613 yr
β_6	p_1	longitude of the Sun's perigee	20,940 yr

As was indicated when comparing Doodson's and Darwin's work, a very important point is that these angular variables are referred to the plane of the ecliptic—the plane created by the orbital motion of the Earth about the Sun. This should be remembered as it will be referred to again when discussing the solid-tide contribution.

3.2 Doodson's Harmonic Representation of Tide Height

Traditionally, as defined by Doodson, the variation in height at tide gages has been represented by an amplitude and associated phase for each argument number. The argument number is a shorthand notation for representing the integral coefficients of the six fundamental figures used to

evaluate the angular argument.

The argument number is obtained by taking the last five integral coefficients and adding the integer 5 to each to create a set of positive integers. This new set of six positive digits then constitutes the argument number. For example, if the angle

$$2\tau - 3s + 4h + p - 2N' + 2p_1$$

is being considered, the argument number that represents this frequency is 229.637. The first three numbers are called the constituent number (229). The first two are called the group number (22), and first number is called the species number (2). Doodson's constituent number and the Darwinian symbols can usually be used to represent the same collection of major frequencies (periods of one year or less).

A breakdown of some of the Darwinian symbols and associated Doodson argument numbers are given in table 3.

Thus, at any tide gage the tide height can be represented by

$$h(T) = \sum_n \delta_n \cos(\overline{n} \cdot \overline{\beta} - \psi_n) \tag{3.1}$$

where $\overline{n} \cdot \overline{\beta} = \sum_{i=1}^{6} n_i \beta_i$. $\overline{n}$ is a vector of the six integers representing all possible combinations of β_i, or what Doodson called the argument number. n_1 is always restricted to positive integers while $n_2 - n_6$ can take on any positive or negative integer value. δ_n and ψ_n are the associated amplitudes and phases at the gage.

This same procedure can be extended to represent amplitude and phase over the entire Earth surface (Hendershott and Munk, 1970)

$$h(\phi, \lambda, T) = \sum_n \delta_n(\phi, \lambda) \cos[\overline{n} \cdot \overline{\beta} - \psi_n(\phi, \lambda)] \tag{3.2}$$

30

Table 3.--Selected Darwinian symbol and Doodson
argument numbers

Darwinian Symbol	Doodson Argument Number	Period (hr)	Description
M_2	255.555	12.42	Principal lunar semi-diurnal
S_2	273.555	12.00	Principal solar semi-diurnal
N_2	245.655	12.66	Larger lunar elliptic semi-diurnal
K_2	275.555	11.97	Luni-solar semi-diurnal
L_2	264.455	12.19	Smaller lunar elliptic
K_1	165.555	23.93	Luni-solar diurnal
O_1	145.555	25.82	Principal lunar diurnal
P_1	163.555	24.07	Principal solar diurnal
Q_1	135.655	26.87	Larger lunar elliptic
Mf	075.555	13.66 d	Lunar fortnightly
Mm	065.455	27.55 d	Lunar monthly
Ssa	057.555	188.62 d	Solar semi-annual

This is accomplished by expressing (3.2) in terms of

$$\delta_n(\phi,\lambda)\cos \psi_n(\phi,\lambda) \text{ and } \delta_n(\phi,\lambda)\sin \psi_n(\phi,\lambda)$$

which are then expressed in series of surface spherical harmonics (Lambeck et al. 1974). Of course, on the continents the $\delta_n(\phi,\lambda)$ must vanish. That is, the height for any frequency component $\bar{n} = (n_1,n_2,\dots,n_6)$ at any point (ϕ,λ), at time T, will be given as

$$h_n(\phi,\lambda,T) = \sum_{\ell=0}^{\infty} \sum_{m=0}^{\ell} P_{\ell m} (\sin \phi) [C^+_{n\ell m} \sin(\bar{n}\cdot\bar{\beta}+m\lambda+\varepsilon^+_{\ell m})$$

$$+ C^-_{n\ell m} \sin (\bar{n}\cdot\bar{\beta} - m\lambda+\varepsilon^-_{\ell m})] \tag{3.3}$$

31

The $\ell = 0, 1$ components of (3.3) are discussed by Hendershott (1972).

3.3 Cotidal Charts

Although the global tide solution is expressed by a set of coefficients $C_{n\ell m}^{+}$ and $C_{n\ell m}^{-}$, scanning this list of coefficients is unacceptable when trying to visualize the physical processes. The traditional method of presenting any ocean tide model is with a cotidal chart. A typical cotidal chart is given in figure 6. The physical features of the global tide are readily available. For example, there are places where no tidal oscillations exist. These points are called amphidromes. The tidal crest will circulate about these amphidromic points with the period of the particular tidal component being investigated. On the cotidal chart the amphidromes can be found where the constant phase lines or cotidal lines emanate. Those lines not originating at the amphidromes are the lines of constant amplitude or corange lines.

3.4 Numerical Solutions of Laplace Tide Equations

It has been tried several times to integrate numerically the Laplace tidal equations using modern computer methods (Hendershott, 1972; Bogdanov and Magarik, 1967; Pekeris and Accad, 1969). To date, no two solutions exhibit close agreement. Large variations in location of amphidromes exist and phase differences of hours are common. Table 4 gives the principal terms in the spherical harmonic representation of three models for the M_2 component as given by Lambeck et al. (1974). Notice that the amplitudes differ by approximately 25%. Disagreement in the phases is also quickly observed. This is not unexpected, however. It was necessary for each investigator to model such characteristics as ocean bottom

32
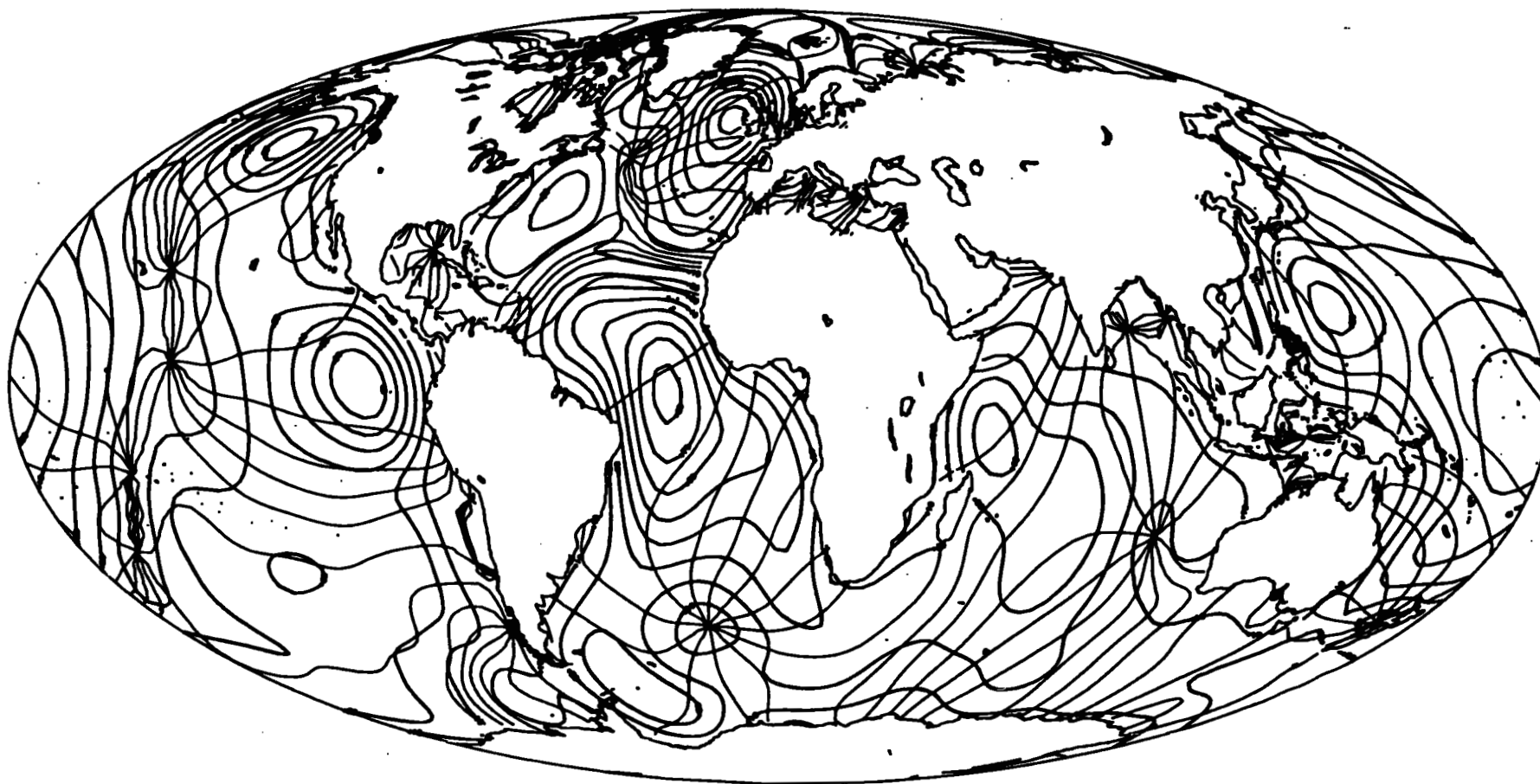
Figure 6.--A Typical Cotidal Chart

topography, coastal boundaries, internal friction due to the viscosity of water, ocean loading and friction in the shallow seas.

3.5 Other Methods for Resolution of Tidal Parameters

One could also suggest that the solution for the phases and amplitudes be obtained from least-squares fits of the spherical harmonic representations to tide gage data. This would be the most obvious method if sufficient data were available from the open areas of the oceans. To date, mostly coastal tide gage data are available, and the dynamics of the tides in these areas is controlled by the coastal boundaries and the continental shelf. A few deep sea instrumental results are indeed available, but not nearly enough to be used to obtain any representation of the global tide. Their use has been restricted to a realistic comparison of solutions of the Laplace tidal equations.

Satellite perturbations, on the other hand, do reveal the effect of global solid and ocean tides. This phenomenon affords us the opportunity to solve for a limited set of spherical harmonic coefficients without having to construct the complicated dynamics required by oceanographers when trying numerically to solve the tidal differential equations.

Table 4.--Principal coefficients from various ocean tide models

Investigator	C_{22}^+ (cm)	ε_{22}^+ (degree)	C_{42}^+ (cm)	ε_{42}^+ (degree)
Pekeris and Accad	4.4	340	1.4	170
Hendershott	5.1	316	1.2	115
Bogdanov and Magarik	4.3	325	1.7	116

34

3.6 Ocean Tide Potential

Once the tide height is known, then the potential due to this mass of
water can be obtained. This is accomplished by realizing that the tidal
layer constitutes a very thin film with constant density and varying height
covering a nearly spherical body. The mass of a small element located at
latitude ϕ and longitude λ on the surface is given by

$$dm(\phi,\lambda) = \sum_n h_n(\phi,\lambda) \, \rho_w \, a_e^2 \cos\phi \, d\phi \, d\lambda \tag{3.4}$$

where the summation is computed over all possible tidal frequencies n.
Integrating the differential external potential due to each differential
mass at (ϕ,λ) over the entire sphere yields a modified or time varying
potential due to this tidal layer on any mass at point (r',ϕ',λ')

$$\Delta U(r',\phi',\lambda',T) = G \int_0^{2\pi} \int_{-\pi/2}^{\pi/2} \frac{\sum_n h_n(\phi,\lambda)\rho_w a_e^2 \cos\phi \, d\phi \, d\lambda}{(r'^2 - 2a_e r'\cos\gamma' + a_e^2)^{\frac{1}{2}}} \tag{3.5}$$

The denominator in (3.5) is just the distance from any point (r',ϕ',λ')
to the differential mass on the surface at (ϕ,λ). γ' is the angle from
(a_e,ϕ,λ) to the center of the Earth to the point (r',ϕ',λ'). Noting that
$(r'^2-2a_e r'\cos\gamma' +a_e^2)^{-\frac{1}{2}}$ is the generating function for Legendre polynomials
and using the orthogonality relation between Legendre polynomials and
associated Legendre functions (which occurs when the tide height representa-
tion is multiplied by the Legendre polynomials generated by the expansion
of the denominator), equation (3.5) can now be written (MacRobert 1967;
Menzel 1961)

$$\Delta U(r',\phi',\lambda',T) = 4\pi G a_e \sum_{n\ell m} \frac{1}{2\ell+1} \left(\frac{a_e}{r'}\right)^{\ell+1} h_{n\ell m}(\phi',\lambda)\rho_w$$

or

$$\Delta U'(r',\phi',\lambda',T) = 4\pi G a_e \rho_w \sum_{n\ell m} \frac{1}{2\ell+1} \left(\frac{a_e}{r'}\right)^{\ell+1} P_{\ell m}(\sin\phi') \cdot \qquad (3.6)$$

$$[C^+_{n\ell m} \sin(\bar{n}\cdot\bar{\beta}+m\lambda'+\epsilon^+_{n\ell m}) + C^-_{n\ell m} \sin(\bar{n}\cdot\bar{\beta}-m\lambda'+\epsilon^-_{n\ell m})]$$

The center of mass attraction of the Earth causes the ocean floor to depress. There is also another deformation due to the attraction on the ocean floor upward toward the tidal layer. The combination of these two deformation results in yet another change to the potential. This further change due to deformation is defined by the load deformation coefficients h'_n and k'_n (Munk and MacDonald 1960). h'_n is used to define the geometric height change as $h'_n \Delta U_n$. As pointed out by Munk and MacDonald, the depression is greater than the uplift, so h'_n and k'_n are negative as might be expected. Thus, the total potential outside the Earth's surface can now be written

$$\Delta U'(r,\phi,\lambda) = \sum_{n\ell m} (1+k'_\ell) \Delta U_{n\ell m}(r,\phi,\lambda) \qquad (3.7)$$

where $\Delta U(r,\phi,\lambda)$ is given in (3.6). The time variable T has been suppressed. Numerical values of k'_n used in this study are taken from Farrell (1972).

$$k'_2 = -0.308$$
$$k'_4 = -0.132$$

Lambeck et al. (1974), following the same procedure as Kaula (1969), have expressed equation (3.7) in terms of the Keplerian (equatorial) elements of a satellite

$$\Delta U' = \frac{4\pi Ga_e^2 \rho_w}{a} \sum_n \sum_\ell \sum_m \sum_p \sum_q \overset{-}{\underset{+}{\sum}} \frac{(1+k_\ell')}{2\ell+1} \left(\frac{a_e}{a}\right)^\ell .$$ (3.8)

$$C_{n\ell m}^{\pm} F_{\ell mp}(i)\ G_{\ell pq}(e) \begin{bmatrix} \pm\sin \\ \\ \mp\cos \end{bmatrix} \begin{matrix} \ell-m \ \text{even} \\ \gamma_{n\ell mpq}^{\pm} \\ \ell-m \ \text{odd} \end{matrix}$$

where $\gamma_{n\ell mpq}^{\pm} = (\ell-2p)\omega + (\ell-2p+q)M + m(\Omega-\theta) \pm \overline{n}\cdot\overline{\beta} \pm \epsilon_{n\ell m}^{\pm}$

The inclination functions $F_{\ell mp}(i)$ and eccentricity functions $G_{\ell pq}(e)$ are the same polynomials discussed in Chapter 2.

3.7 Analytic Approximations of Ocean Tide Perturbations

As with estimating perturbations due to the geopotential, the potential $\Delta U'$ must be substituted into the Lagrangian planetary equations to obtain the six first-order differential equations of the motion. Again, noting that a,e,i remain nearly constant, the integration of these equations can be approximated by assuming the angular variables Ω,ω,M,β_i to change linearly in time (i.e., secular rates due to C_{20} are used for $\dot\Omega,\dot\omega,\dot M$). Now the differential equations are easily integrated. For example, the inclination perturbations are given by

$$\Delta i_{n\ell mpq}^{\pm} = \frac{4\pi(1+k_\ell')}{2\ell+1}\ Ga_e\left(\frac{a_e}{a}\right)^{\ell+1} \frac{\rho_w}{Na^2(1-e^2)^{1/2}\sin i}\ C_{n\ell m}^{\pm}\ F_{\ell mp}(i)\ G_{\ell pq}(e)$$ (3.9)

$$\left[\frac{(\ell-2p)\cos i - m}{\dot\gamma^{\pm}}\right]\begin{bmatrix} \pm\sin \\ \\ \mp\cos \end{bmatrix} \begin{matrix} \ell-m \ \text{even} \\ \gamma_{n\ell mpq}^{\pm} \\ \ell-m \ \text{odd} \end{matrix}$$

Notice the presence of the $\dot{\gamma}^{\pm}$ in the denominator of (3.9). Since the perturbations due to ocean tides are small, small values of $\dot{\gamma}^{\pm}$ will be required to amplify the perturbations to a detectable level. It is for this reason that mean elements (slowly varying) rather than osculating elements are analyzed.

Integration of the node is slightly more complicated. There is the expected 'direct' effect and an indirect effect through the C_{20} secular rate assumption. First, the direct effect is found by integration of the $\dot{\Omega}$ equation, as was done for di/dt. This indirect effect is obtained by realizing that the assumed secular rate due to C_{20}

$$\dot{\Omega}_{secular} = \frac{3 \sqrt{\frac{\mu}{a^3}} \, C_{20} \, a_e^{\,2}}{2(1-e^2)^2 \, a^2} \cos i$$

will experience small changes due to the low frequency variation in the inclination obtained in equation (3.9). Thus, the indirect effect is

$$\Delta\Omega(t)_{indirect} = \int \frac{\partial \dot{\Omega}_{secular}}{\partial i} \, \Delta i(t) \, dt.$$

Combining these two effects gives

$$\Delta\Omega^{\pm}_{n\ell mpq} = \frac{4\pi(1+k'_\ell)}{2\ell+1} \, Ga_e\left(\frac{a_e}{a}\right)^{\ell+1} \frac{\rho_w}{Na^2(1-e^2)^{\frac{1}{2}}\sin i} \, C^{\pm}_{n\ell m} \, G_{\ell pq}(e) \, \frac{1}{\dot{\gamma}^{\pm}} \left\{ \frac{\partial F_{\ell mp}(i)}{\partial i} \right. -$$

$$(3.10)$$

$$\left. \frac{3}{2}N\left(\frac{a_e}{a}\right)^2 \frac{C_{20}\sin i}{(1-e^2)^2} \, F_{\ell mp}(i) \, \frac{[(\ell-2p)\cos i - m]}{\dot{\gamma}^{\pm}} \right\} \begin{bmatrix} \mp\cos \\ \mp\sin \end{bmatrix}^{\ell-m \text{ even}}_{\ell-m \text{ odd}} \gamma^{\pm}_{n\ell mpq}$$

38

3.8 Long Period Ocean Tide Perturbations

For a given vector of coefficients $\bar{n}$, only certain values of ℓmpq are admissible to achieve low frequency perturbations (periods longer than one day). $\ell - 2p + q$ must equal zero to eliminate the mean anomaly. Since $\dot{\beta}_1 = \dot{\theta} - \dot{s}$, where $\dot{\theta}$ is the sidereal rotation, n must equal n_1 to cancel out all daily variations. m cannot take on negative values so only angular variables γ^+ yield long period terms. Since perturbations are proportional to $e^{|q|}$, q must equal zero to rule out negligible terms. With q set equal to zero, the $\ell - 2p + q$ coefficient now reduces to $\ell - 2p$. Thus ℓ must now be even. For semidiurnal terms ($n_1 = 2$), values of ℓ and m to be considered are $(2,2)$, $(4,2)$, $(6,2)$.... For the diurnal tides ($n_1 = 1$), ℓ and m can take on the values $(2,1)$, $(4,1)$, $(6,1)$.... Only $\ell = 2,4$ need be considered.

To sense the magnitude of these ocean tide perturbations, table 5 gives amplitude estimates on the inclination and node elements for several satellites. One notices at once the large perturbations due to solar tides. As was pointed out previously, this effect is due to the small values of γ which appear in the denominator of the perturbation equations. It is also obvious that the perturbation due to the tidal component, which is the most desirable to observe, makes the principal lunar semidiurnal or M_2, in fact, one of the most difficult to resolve. From table 5 it is seen that resolution of the M_2 ocean tide requires an accuracy of 2/100 arc second in the node and inclination data. The data of Douglas et al. (1972) were accurate to the 1/10 arc second level which enables them to resolve the much larger solid-tide perturbations.

Table 5.—Predicted perturbations on several satellites

Satellite	M$_2$			O$_1$			S$_2$			P$_1$		
	Δi (arc sec)	ΔΩ (arc sec)	Period (days)	Δi (arc sec)	ΔΩ (arc sec)	Period (days)	Δi (arc sec)	ΔΩ (arc sec)	Period (days)	Δi (arc sec)	ΔΩ (arc sec)	Period (days)
GEOS-1 (i=59.4°)	0.03	0.01	11.7	0.00	0.00	12.6	0.04	0.05	55.7	0.06	0.01	85.4
GEOS-2 (i=105.8°)	.04	.02	15.3	.00	.01	14.4	.43	2.70	432.3	.28	3.33	632.4
GEOS-3 (i=115.0°)	.06	.03	17.2	.00	.01	15.2	.12	.26	103.9	.41	2.52	482.1
NAVSAT (i=89.25°)	.04	.01	13.6	.00	.01	13.6	.20	.54	169.6	.00	.31	175.9
BE-C (i=41.2°)	.04	.03	10.3	.01	.01	11.8	.03	.04	34.4	.07	.07	57.9
STARLETTE (i=49.8°)	.04	.04	10.5	.01	.01	11.9	.03	.05	36.5	.08	.03	60.8
SEASAT (i=108.0°)	.07	.03	16.2	.00	.01	14.8	.21	.68	163.4	2.	108.	3120.
LAGEOS (i=110.0°)	.01	.00	14.0	.00	.00	13.8	.05	.02	280.7	.02	.07	221.3

4. SOLID TIDE

4.1 Tide Raising Potential

Based on Newton's inverse square theory of gravitation, the attraction of the Sun on the Earth is approximately 178 times the attraction of the Moon on the Earth. However, the origin of the tidal forces is due to the difference of attractions of the body at any point on the surface with the same attraction at the center of mass. On figure 7, the gravitational forces (Newtonian attraction) are represented by the solid lines. Differencing the force on the center of mass with the other two forces at the surface (solid lines) yields the origins of the body and ocean tides (in conjunction with the Earth's rotation) represented by the dotted lines. Thus, the tidal forces are proportional to the inverse cube of the distance to the disturbing body. It then follows that the lunar tidal force is actually about twice the solar tidal force due to the proximity of the Moon to the Earth.

A deformation is created by this attraction which looks like an ellipsoid with the major axis pointing toward the Moon.

The gravitational acceleration of a mass m^* at a point $\overline{r}^*$ on mass at point $\vec{r}$ relative to the center of the Earth can be calculated from its corresponding potential

$$U = Gm^* \sum_{n=2}^{\infty} \frac{r^n}{r^{*n+1}} \; P_n (\cos s) \qquad (4.1)$$

where $\cos s = \dfrac{\overline{r} \cdot \overline{r}^*}{|\overline{r}| \; |\overline{r}^*|}$, the cosine of the angle from the mass point to the disturbing body from the center of the Earth.

41
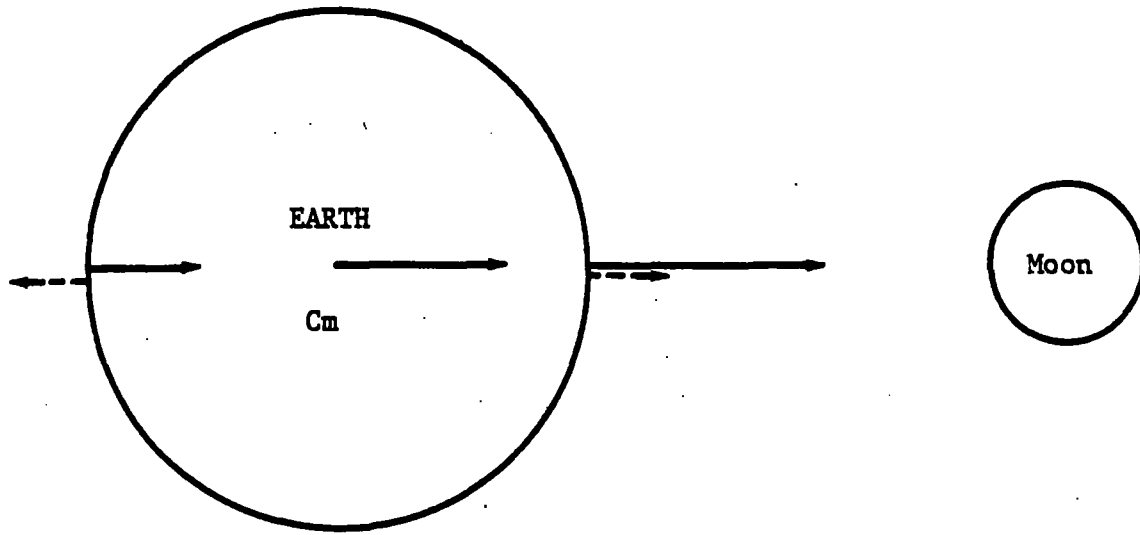
Figure 7.—Tide Raising Forces Due to the Moon

As with the loading due to the ocean tides discussed in the previous chapter, proportionality constants (called Love numbers) are used to represent the height change and associated nonstationary character of the potential due to this attraction. The deformation in height for the degree n at the surface is defined by $h_n U_n(a_e)/g$. The modification to the potential at the surface is defined by the potential Love numbers, k_n, as

$$\Delta U(a_e) = \frac{Gm^*}{r^*} \sum_{n=2}^{\infty} k_n (\frac{a_e}{r^*})^n P_n(\cos s) \qquad (4.2)$$

Since the moon is at approximately 60 Earth radii from the Earth, increasing the degree of n results in a damping effect of 1/60.

Applying Dirichlet's theorem allows one to calculate the additional potential outside the Earth due to this deformation as

$$\Delta U(r) = \frac{Gm^*}{r^*} \sum_{n=2}^{\infty} k_n \left(\frac{a_e}{r^*}\right)^n \left(\frac{a_e}{r}\right)^{n+1} P_n (\cos s). \qquad (4.3)$$

4.2 Solid Tide Potential as a Function of Satellite Keplerian Elements

Kaula (1969) has reformulated the above in terms of the Keplerian elements of both the disturbing body and the mass as

$$\Delta U = Gm^* \sum_{n=2}^{\infty} \sum_{m=0}^{n} \sum_{p=0}^{n} \sum_{q=-\infty}^{\infty} \sum_{h=0}^{n} \sum_{j=-\infty}^{\infty} k_n \left(\frac{a_e}{a}\right)^{n+1} \kappa_m \frac{(n-m)!}{(n+m)!} \frac{a_e^n}{a^{*\,n+1}}$$

$$F_{nmp}(i) \, F_{nmh}(i^*) \, G_{npq}(e) \, G_{nhj}(e^*) \, \cos[(n-2p)\omega+(n-2p+q)M \qquad (4.4)$$

$$-(n-2h)\omega^*-(n-2h+j)M^*+m(\Omega-\Omega^*)]$$

$$\kappa_m = \begin{cases} 1 & m=0 \\ 2 & m \neq 0 \end{cases}$$

where F(i) and G(e) are the familiar inclination and eccentricity polynomials.

Normally the coordinate system in which the above Kepler elements are referenced is an Earth equatorial system. However, as previously discussed, the historical representation of the ocean tides has been in terms of the ecliptic variables of the disturbing body (Moon or Sun). This is only natural since the mean angular rates of the Moon or Sun are rather constant and also well known in the ecliptic system. On the other hand, the system in which satellite mean element rates are fairly constant is the Earth

equatorial system. This too is only natural since the major perturbing effect on near Earth satellites is due to the Earth's oblateness. Thus, in order to compare in detail the effects of both solid and fluid tide perturbations, it is necessary to express the disturbing potential in terms of the satellite equatorial elements and the body's ecliptic elements.

The mechanics of this transofrmation can be found in appendix I. The resultant form of the potential in terms of the equatorial elements of the satellite and ecliptic elements of the disturbing body is given bv

$$\Delta U = Gm^* \sum_{n=2}^{\infty} \sum_{m=0}^{n} \sum_{p=0}^{n} \sum_{q=-\infty}^{\infty} \sum_{k=-n}^{n} \sum_{h=0}^{|k|} \sum_{j=-\infty}^{\infty} k_n \left(\frac{a_e}{a}\right)^{n+1} \psi^*_{nmk} \frac{a_e^n}{a^{*n+1}} \kappa_m$$ (4.5)

$$\frac{(n-m)!}{(n+m)!} F_{nmp}(i) F_{n|k|h}(i^*) G_{npq}(e) G_{nhj}(e^*) \begin{bmatrix} \cos \\ (-1)^{n-k}\sin \end{bmatrix} \begin{matrix} m-k \text{ even} \\ \rho \\ m-k \text{ odd} \end{matrix}$$

$\rho = (n-2p)\omega + (n-2p+q)M + m\Omega - (n-2h+j)M^* - (n-2h)\omega^* - |k|\Omega^* + \text{sgn}(k)(k-m)\pi/2$.

It is seen that equation (4.5) is very similar to equation (4.4), as would be expected. The extra subscript k simply reflects the fact that the equatorial rates of the disturbing body do vary depending on the alignment in ecliptic space. For example, the equatorial value of the lunar inclination will vary between 18° and 28° depending on the location of the ecliptic value of the node. The ecliptic inclination of approximately 5° will sinusoidally vary about the obliquity of the ecliptic (23°). Likewise, the equatorial node and perigee rates of the disturbing body also vary. The $\psi^*_{n,m,k}$ scale the individual frequency terms. It is

44

also a convenient procedure to equate common frequency components of the solid Earth and ocean tide potentials. Notice also the presence of multiple solid Earth tide terms for a given ocean tide component. For example, the condition for an M_2 term is that the angle $2(\Omega-\Omega^*)-2M^*-2\dot{\omega}^*$ be present. This can happen for two sets of coefficients

$$k = m = 2$$

$$k = -m = -2$$

However, as is pointed out in appendix I, the scale coefficient for $k = -m$ is negligible while for $k = m$ the coefficient is close to unity.

Thus, for each solid tidal component of the potential there is a corresponding ocean tide potential contribution with the same angular argument and vice versa. Another important case is when the degree and order subscripts of the ocean tide terms are equal ($\ell = m$). In this situation the corresponding solid tide component of same frequency will have identical dependence on the satellite orbit. That is, the ratio of the coefficients of the trigonometic functions of the solid and ocean tide terms will be constant no matter what values of a,e,i are used. Thus, the solid and ocean tide parameters cannot be separated from analysis of long period perturbation of orbital elements alone.

4.3 Solid Tide Lag

Since the longest period of free oscillation (Jefferies 1970) of the Earth is slightly less than one hour, we have been able to treat the Earth's response to the deforming attraction as a static response. Because of the anelasticity of the Earth, the actual deformation or rise and fall

in the surface occurs slightly after the point on the surface passes under

the disturbing body. Thus, the potential must be modified slightly to

account for this phenomenon. Following Kozai (1965), let us assume a

modified or fictitious position for the disturbing body under which the

maximum bulge occurs. Figure 8 shows that one must move from point A to

point B. First, any lag in the Earth's response will occur in the direc-

tion of the Earth's rotation. Let Δt be the lag in time (a positive

number). This fictitious position can be represented by a rotation of

the body's orbital plane about the Earth's rotational axis, an amount

$\dot{\theta}\Delta t$, and then backing up the satellite in time, an amount Δt. This pro-

cedure is accomplished by increasing the nodal crossing, an amount $\dot{\theta}\Delta t$,

and then decreasing the mean anomaly by $\dot{M}\Delta t$ or

$$\Omega_f^* = \Omega^* + \dot{\theta}\Delta t \qquad\qquad M_f^* = M^* - \dot{M}^*\Delta t$$

Then a more realistic expression for the disturbing potential can be given

by substituting the above into equation (4.4)

$$\Delta U_{nmpqhj} = k_n \left(\frac{a_e}{a}\right)^{\ell+1} \frac{a_e^n}{a_*^{n+1}} \kappa_m \frac{(n-m)!}{(n+m)!} F_{nmp}(i)\ F_{nmh}(i^*)\ G_{npq}(e)\ G_{nhj}(e^*)$$

$$\text{(4.6)}$$

$$\cos[(n-2p)\omega+(n-2p+q)M-(n-2h)\omega^*-(n-2h+j)M^*+m(\Omega-\Omega^*)+\varepsilon_{\ell mhj}]$$

where $\varepsilon_{\ell mhj} = -(n-2h+j)\dot{M}^*\Delta t + m\dot{\theta}\Delta\tau$

$\approx m\dot{\theta}\Delta t$

$\Delta t = \dfrac{\delta_2}{\dot{\theta}} = \ell ag/\text{Earth's rotation}$

This approach agrees with Newton (1968) and Kaula (1969) in that the lag

angle is proportional to frequency (Darwinian assumption).
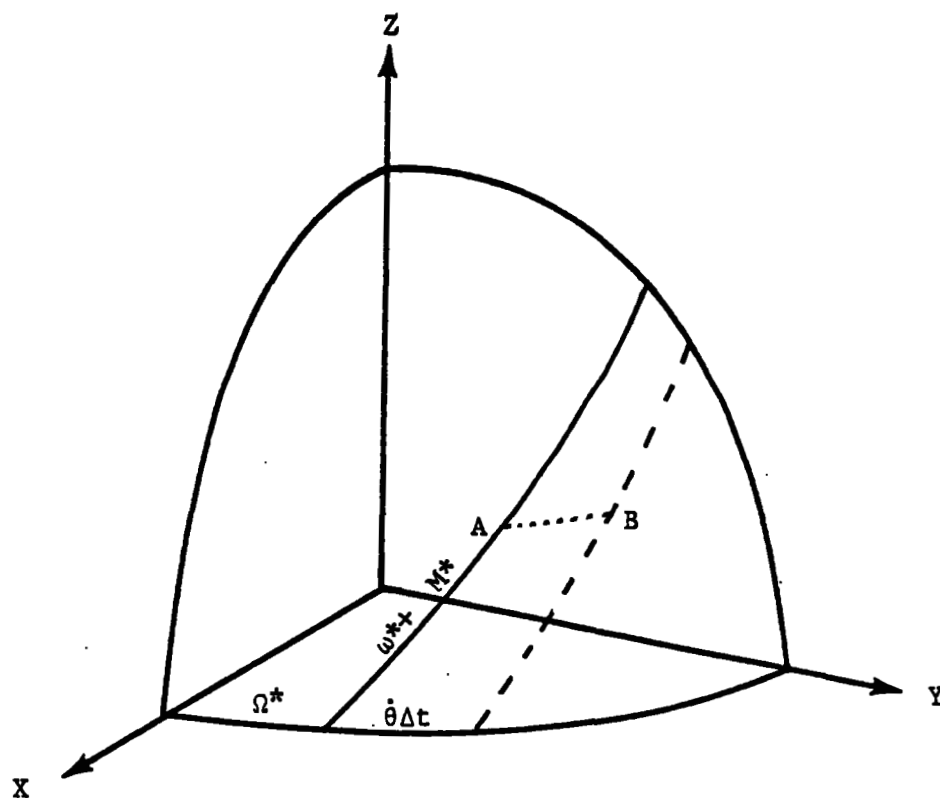
Figure 8.--Fictitious Lunar Orbit Compensation for Solid Earth Phase Lag

5. ESTIMATION OF M_2 OCEAN TIDE PARAMETERS FROM SATELLITE ORBIT PERTURBATIONS

5.1 Discussion of Data

Two histories of satellite ephermerides have been obtained for studying the effects of solid and ocean tides. The first was a set of osculating elements of a U. S. Navy Navigation satellite 1967-92A obtained from James G. Marsh of the NASA's Geodynamics Branch, Goddard Space Flight Center, Greenbelt, Maryland. Mr. Marsh obtained the Doppler data for this satellite covering a 160-day arc from the U. S. Department of Defense.

The second satellite for which data were made available is the GEOS-3 satellite. GEOS-3 was launched in early 1975 and was designed specifically for geodetic investigations. It is the first satellite launched with an operational radar altimeter (NASA , 1974) to measure directly the surface of the oceans. To be able to utilize the high quality altimeter data, the Naval Surface Weapons Center, Dahlgren, Virginia tracked GEOS-3 with approximately 40 globally distributed Doppler stations on a continual basis. Very precise orbits were obtained from this tracking campaign. Using the mean element conversion program, which was created for this study, the Defense Mapping Agency Topographic Center, Washington, D. C. converted a 200-day arc of osculating GEOS-3 data for use in this endeavor.

5.2 Analysis of 1967-92A Satellite

The gravity model used by Marsh when determining the orbits of 1967-92A from the Doppler data was the GEM-7 model (Wagner et al. 1976). The use of GEM-7 was an important factor in the success of this work. In order to

achieve a precision of 0.01 arc seconds, it was necessary to consider

perturbations due to the entire GEM-7 model (which is complete to 25,25)

and remove about 600 ℓmpq terms in Kaula's formulation of geopotential

perturbations.

Table 6 gives the expected perturbations on 1967-92A due to different

tidal components. Of course, the M_2 tide is the one currently being

sought. Remembering that the tidal amplitude is proportional to the

period (inversely proportional to the rate), it is reasonable to expect

the solar tides to be larger in amplitude than the lunar ones. For 1967-

92A the node is rather insensitive to either the (2,2) or the (4,2) tidal

harmonics. It is for this reason that only the inclination of 1967-92A

is studied.

After the 1967-92A mean elements were passed through the ROAD program,

the differences between the theoretical orbit, which ROAD determined from

the data, and actual mean elements were output for further analysis.

The inclination differences were then assumed to have the ocean tide

perturbations and solid tide errors remaining, since it was unmodeled in

the ROAD computer runs. Also, other unmodeled or mismodeled effects were

also left behind. Therefore, it was necessary to extract the ocean tide

perturbations using standard least-squares procedures. An amplitude and

phase were fitted to the inclination residuals at the M_2 frequency as

well as other frequencies which appeared, such as resonant, S_2, P_1 fre-

quencies. A slope and an intercept were also included in the solution

set to remove left-over secular and very long period effects, such as

the K_1 and K_2 tidal effects. A periodic effect of unknown origin, with a

period equal to approximately 8 days, also had to be included in the

solution set.

Figure 9 shows a typical portion of the inclination residuals after removing all perturbations including solid tide effects with k_2 = 0.30 and δ = 0° except for the solved-for amplitude and phase at the M_2 frequency. Not the M_2 tide is clearly discernible. The rms fit to the data was 0.03 arc seconds. The solution for amplitude and phase at the M_2 frequency implies the following observation equation for the M_2 tide:

$$(3\overset{''}{.}8 \pm .60) \times 10^{-2} \sin [\sigma(t)+331^\circ \pm 10^\circ] =$$

$$\frac{0\overset{''}{.}99}{cm} \times 10^{-2} \; c_{22}^+ \; \sin[\sigma(t)+\varepsilon_{22}^+] + \frac{0\overset{''}{.}94}{cm} \times 10^{-2} \; c_{42}^+ \; \sin[\sigma(t)+\varepsilon_{42}^+]$$

(5.1)

where $\sigma(t)$ = $2\Omega - 2M* - 2\omega* - 2\Omega*$

Table 6.—Perturbations on the inclination of 1967-92A
satellite due to ocean tides

Component	Period Days	Amplitude	Source
M_2	13.6	$0\overset{''}{.}04$	Hendershott* (1972)
S_2	169.6	$0\overset{''}{.}17$	Bogdanov and Magarik* (1967)
K_2	2383.0	Unknown	-----
O_1	13.6	$0\overset{''}{.}000$	Dietrich* (1944)
P_1	175.9	$0\overset{''}{.}004$	Felsentreger et al. (1976)
K_1	4766.0	$0\overset{''}{.}08$	Dietrich* (1944)

*As reported by Lambeck et al. (1974).
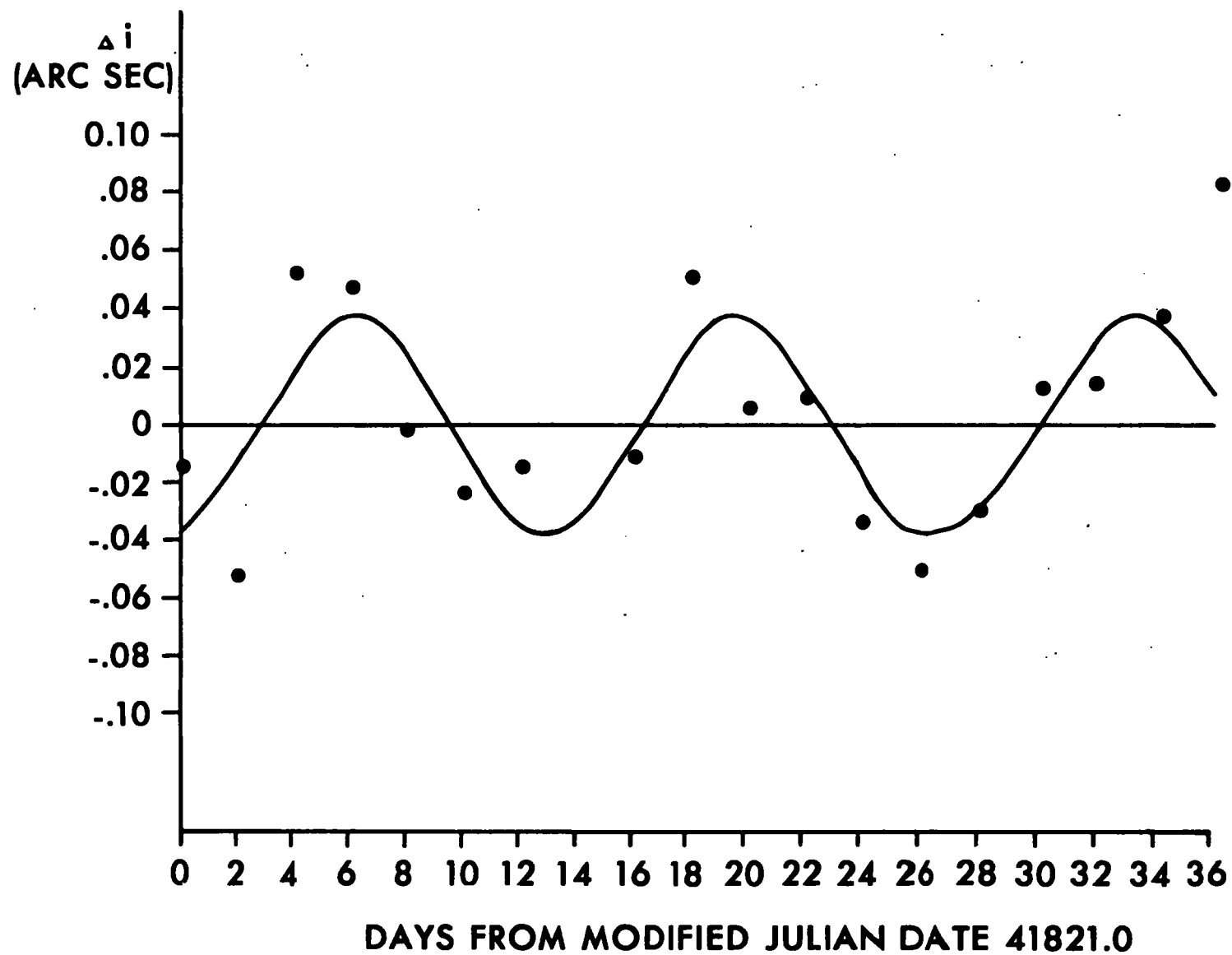
Figure 9.--Observed versus calculated inclination values at M_2 frequency for 1967-92A.

$\sigma(t)$ is equal to 1 cycle/13.58 days.

Table 7 gives a comparison of this result with amplitude and phase predicted from four other numerical M_2 tide results. The mean elements used to obtain these results are given in table 8.

The formal variances of these results were obtained by assuming the variance of the data to be equal to the mean squared residual after the fit (0."03). Because of the uniqueness of the M_2 frequency (the effect of the O_1 component is negligible on 1967-92A), little aliasing from other sources is likely. Thus, the formal uncertainties obtained are reasonably reliable.

Of course, other tidal components can also be obtained from these mean elements, but caution is required because of aliasing effects.

Table 7.—Amplitude and phase of inclination perturbations
due to the M_2 ocean tide on 1967-92A satellite

Source	Amplitude	Phase
Observed	0."038	$331°$
Pekeris and Accad	0."031	$335°$
Hendershott (Model 1)	0."040	$322°$
Hendershott (Model 2)	0."044	$280°$
Bogdanov and Magarik	0."030	$340°$

5.3 Analysis of GEOS-3 Satellite

GEOS-3 is an ideal satellite to use for tidal studies. For M_2 recovery, the inclination perturbation is dominated by the (2,2) harmonic and the

Table 8. Mean Keplerian Elements (1967-92A)

TIME (MJD)	A (METERS)	E	I (DEGREES)	NODE (DEGREES)	PERIGEE (DEGREES)	M (DEGREES)
41821.0	7450987.486	0.0053695	89.24673344	36.97650888	24.76178357	56.59259076
41823.0	7450986.885	0.0052570	89.24602235	36.82450599	19.52975786	49.11872932
41825.0	7450985.847	0.0051408	89.24562807	36.67228158	14.18980869	41.75514648
41827.0	7450985.042	0.0050212	89.24568904	36.52015004	8.73695363	34.50651422
41829.0	7450983.963	0.0048994	89.24612784	36.36823880	3.15397258	27.38920763
41831.0	7450983.128	0.0047762	89.24652640	36.21655193	357.43684894	20.40681731
41833.0	7450982.345	0.0046534	89.24631777	36.06488154	351.56661857	13.57846940
41835.0	7450981.841	0.0045324	89.24541867	35.91280483	345.53396566	6.91426227
41837.0	7450981.196	0.0044142	89.24456488	35.76027840	339.32532836	0.42852212
41839.0	7450980.524	0.0043007	89.24440287	35.60770861	332.93320062	354.12832147
41841.0	7450980.050	0.0041931	89.24476871	35.45545186	326.35789922	348.01209787
41843.0	7450979.297	0.0040933	89.24516443	35.30341585	319.60044007	342.07820769
41845.0	7450978.480	0.0040032	89.24511177	35.15147979	312.65679814	336.33119465
41847.0	7450977.735	0.0039236	89.24463201	34.99932275	305.53045712	330.76854172
41849.0	7450977.051	0.0038567	89.24386303	34.84687105	298.24330748	325.36868149
41851.0	7450976.386	0.0038037	89.24320800	34.69416913	290.82288221	320.10417888
41853.0	7450975.487	0.0037657	89.24295417	34.54133560	283.29377124	314.95041475
41855.0	7450974.787	0.0037438	89.24318343	34.38865344	275.68676056	309.87612131
41857.0	7450973.971	0.0037375	89.24365504	34.23622701	268.03932025	304.84310568
41859.0	7450973.166	0.0037480	89.24385106	34.08397817	260.39851613	299.80410601
41861.0	7450972.361	0.0037749	89.24337556	33.93155827	252.80699106	294.71721456
41863.0	7450971.578	0.0038174	89.24244006	33.77867256	245.30185636	289.54628612
41865.0	7450970.954	0.0038746	89.24183541	33.62545804	237.90443505	284.27045135
41867.0	7450970.132	0.0039454	89.24200596	33.47234568	230.65788926	278.84515349
41869.0	7450969.411	0.0040282	89.24260460	33.31959848	223.58572635	273.24591463
41871.0	7450968.572	0.0041217	89.24295119	33.16712452	216.68990291	267.47095648
41873.0	7450968.091	0.0042241	89.24281676	33.01458716	209.98679512	261.50423650
41875.0	7450967.583	0.0043336	89.24227439	32.86183592	203.46728445	255.35542974
41877.0	7450967.170	0.0044485	89.24166190	32.70878150	197.13450870	249.02168640
41879.0	7450966.550	0.0045670	89.24133077	32.55553882	190.98363954	242.50784111
41881.0	7450965.819	0.0046890	89.24149613	32.40241411	184.99968052	235.82860832
41883.0	7450965.249	0.0048115	89.24206449	32.24942558	179.17202591	228.99370399
41885.0	7450964.424	0.0049347	89.24266275	32.09684095	173.49198324	222.01149817
41887.0	7450963.858	0.0050557	89.24283512	31.94433296	167.95572219	214.88606566
41889.0	7450963.158	0.0051745	89.24237623	31.79158588	162.54823510	207.63343500
41891.0	7450962.773	0.0052897	89.24169930	31.63845407	157.24553134	200.27831087
41893.0	7450962.306	0.0054011	89.24162348	31.48512758	152.04475149	192.82332969
41895.0	7450961.562	0.0055069	89.24230245	31.33216065	146.93867214	185.27461460
41897.0	7450960.708	0.0056064	89.24319457	31.17955849	141.92319311	177.63582150
41899.0	7450960.033	0.0056987	89.24362340	31.02721463	136.97397750	169.93118385
41901.0	7450959.544	0.0057845	89.24357442	30.87479097	132.08857717	162.16373898
41903.0	7450959.087	0.0058622	89.24325479	30.72213297	127.26076741	154.34008662
41905.0	7450958.629	0.0059308	89.24300209	30.56929234	122.47758164	146.47337846
41907.0	7450958.140	0.0059909	89.24314149	30.41646811	117.74101522	138.56165929
41909.0	7450957.692	0.0060420	89.24379047	30.26384047	113.03755538	130.61771890
41911.0	7450957.475	0.0060841	89.24471775	30.11159738	108.36151017	122.64643278
41913.0	7450956.899	0.0061160	89.24543726	29.95952159	103.70221815	114.65821152
41915.0	7450956.498	0.0061378	89.24556579	29.80754180	99.06323876	106.65020716
41917.0	7450956.243	0.0061502	89.24516646	29.65535827	94.43538724	98.63234616
41919.0	7450955.832	0.0061531	89.24490943	29.50284086	89.81685561	90.60702596
41921.0	7450955.305	0.0061456	89.24534764	29.35033637	85.19185229	82.58952259
41923.0	7450954.562	0.0061274	89.24639485	29.19835620	80.55373675	74.58556980
41925.0	7450953.966	0.0060997	89.24731839	29.04678026	75.90402237	66.59330899
41927.0	7450953.544	0.0060631	89.24768625	28.89528258	71.23603296	58.61977920
41929.0	7450953.130	0.0060172	89.24758828	28.74368715	66.54387735	50.67157340
41931.0	7450952.489	0.0059618	89.24736511	28.59190841	61.81685696	42.76004739
41933.0	7450951.747	0.0058973	89.24736914	28.44001089	57.04790620	34.89249409
41935.0	7450951.224	0.0058244	89.24779497	28.28822276	52.23666887	27.06869958
41937.0	7450950.413	0.0057439	89.24869960	28.13667402	47.37956612	19.29162646
41939.0	7450949.846	0.0056559	89.24965408	27.98556702	42.45836269	11.57880764
41941.0	7450949.187	0.0055607	89.25012688	27.83461826	37.46732785	3.93611291
41943.0	7450948.725	0.0054589	89.24998287	27.68355747	32.39894669	356.37195919
41945.0	7450948.463	0.0053517	89.24957656	27.53223383	27.25161052	348.88866719
41947.0	7450947.896	0.0052397	89.24958327	27.38068702	22.00678244	341.50473828
41949.0	7450947.040	0.0051239	89.25029316	27.22941743	16.64640304	334.23776055
41951.0	7450946.009	0.0050052	89.25130384	27.07854991	11.16885466	327.08885407
41953.0	7450944.995	0.0048845	89.25196591	26.92794376	5.57547850	320.05677970
41955.0	7450943.965	0.0047630	89.25204665	26.77740905	359.84756374	313.16075720
41957.0	7450943.164	0.0046420	89.25174556	26.62664355	353.96004543	306.42646759
41959.0	7450942.048	0.0045232	89.25144333	26.47570760	347.90829612	299.85907272
41961.0	7450941.210	0.0044075	89.25143885	26.32466887	341.68758120	293.46313887
41963.0	7450940.485	0.0042962	89.25193779	26.17379285	335.29986968	287.23584531
41965.0	7450939.632	0.0041909	89.25271814	26.02323725	328.73226428	281.18936605
41967.0	7450938.726	0.0040934	89.25336045	25.87294330	321.97517678	275.33314474
41969.0	7450937.909	0.0040055	89.25337433	25.72268701	315.03311959	269.66303230
41971.0	7450937.307	0.0039278	89.25279222	25.57210112	307.92620825	264.16173400
41973.0	7450936.499	0.0038622	89.25224479	25.42123337	300.66203899	258.81615764
41975.0	7450935.391	0.0038108	89.25236656	25.27031938	293.26046094	253.61242273
41977.0	7450934.314	0.0037745	89.25299799	25.11969774	285.74947448	248.51963060
41979.0	7450933.239	0.0037531	89.25361948	24.96940086	278.17114838	243.49514923
41981.0	7450932.335	0.0037473	89.25376882	24.81922158	270.56502738	238.49982493

nodeisaffected mainly by the (4,2) harmonic. The node and inclination data were treated in the same manner as 1967-92A. An amplitude and phase at the M_2 frequency were obtained for each element history. The resulting M_2 observation equations for GEOS-3 are

Inclination :

$$(3.\overset{''}{99} \pm 0.4) \times 10^{-2} \sin [\sigma(t) + 327^{\circ} \pm 4^{\circ}] \qquad (5.2)$$

$$= \frac{1.\overset{''}{26}}{cm} \times 10^{-2} C_{22}^{+} \sin [\sigma(t) + \epsilon_{22}^{+}] - \frac{0.\overset{''}{32}}{cm} \times 10^{-2} C_{42}^{+} \sin [\sigma(t) + \epsilon_{42}^{+}]$$

Node :

$$(2.\overset{''}{73} \pm 0.7) \times 10^{-2} \cos [\sigma(t) + 291^{\circ} \pm 13^{\circ}] \qquad (5.3)$$

$$= - \frac{0.\overset{''}{24}}{cm} \times 10^{-2} C_{22}^{+} \cos [\sigma(t) + \epsilon_{22}^{+}] - \frac{3.38}{cm} \times 10^{-2} C_{42}^{+} \cos [\sigma(t) + \epsilon_{42}^{+}]$$

where $\sigma(t) = 2\Omega - 2M* - 2\omega* - 2\dot{\Omega}*$. $\dot{\sigma}(t)$ is equal to 1 cycle/17.2 days.

The node and inclination histories were considered independently. Since each of the 100 pairs of inclination and node values was the result of a single orbit determination, then it is possible for the element pairs to be highly correlated. Three typical correlation coefficients from different data reductions have been obtained from the Naval Surface Weapons Center (NSWC), Dahlgren, Virginia

$$-0.026$$
$$-0.039$$
$$-0.036$$

These correlation coefficients are quite low. Therefore, using the inclination and node data as if they were independent is justified. Unlike 1967-92A, the node rate on GEOS-3 is not small. Thus, the frequency of

54

perturbations on GEOS-3 of the many tidal constituents will not have a very long or secular trend. Table 9 gives the expected amplitude and associated frequency of the major tidal components. All these terms were included in the least squares adjustment for the M_2 tidal components. An unknown component with a 12.4-day period also had to be included in the solution set.

Table 9.--Perturbations on the inclination and node of
GEOS-3 satellite due to ocean tides

Component	Period Days	Amplitude Inclination	Node	Source
M_2	17.2	0."06	0."03	Hendershott* (1972)
S_2	103.9	."12	."26	Bogdanov & Magarik (1967)*
K_2	66.23	—	--	----
O_1	15.23	."004	."01	Dietrich* (1944)
P_1	482.12	."41	2."5	Felsentreger et al. (1976)
K_1	132.45	."07	."05	Dietrich* (1944)

* As given by Lambeck et al. (1974)

The rms of the fit to the inclination residuals was 0.02 arc seconds; the rms of the fit to the node residuals was 0.04 arc second. The fit of the node is not expected to be as good as the inclination. During each two-day orbital reduction the set of all station longitudes must be modified for any disturbance in time. UT1 corrections used in the data reductions at NSWC - Dahlgren were not available for this study. Figure 10 shows the

55

ARC SEC × 100

9.
6.
3.
0.
-3.
-6.
-9.

42525.   42555.   42585.   42615.   42645.   42675.   42705.

MODIFIED JULIAN DAY
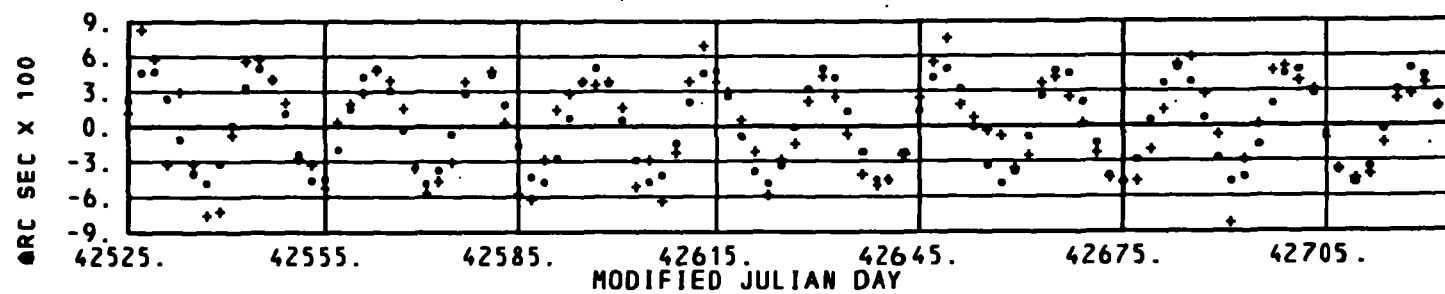
Figure 10.—Observed versus Calculated Inclination Values
at M_2 Frequency for GEOS-3

. - calculated

+ - observed

inclination residuals after removing all perturbations except for the M_2 parameters plotted against the recovered M_2 signal. The presence of the M_2 perturbations is obvious. Table 10 gives a comparison of the recovered M_2 amplitude and phase with the predicted values from the available numerical tide models. Table 11 gives the GEOS-3 mean element data used in the study.

5.4 Two Satellite Least-Squares Ocean Tide Solution

The resulting data reductions have made available three M_2 observation equations for two harmonics - (2,2) and (4,2). Since more observation equations are available than there are unknowns, and since uncertainties are available for each observation, a weighted least-squares solution for the tidal parameters is in order.

Given a linear relationship between a set of measurements Y and a solution state x

$$Y = Ax + \eta$$
$$E(\eta\eta^T) = \Sigma \qquad\qquad (5.4)$$
$$E(\eta) = 0$$

Then the minimum-variance solution is the least-squares solution

$$\hat{x} = [A^T\Sigma^{-1}A]^{-1}A^T\Sigma^{-1}Y \qquad\qquad (5.5)$$

The covariance matrices for the measurements Σ are available from the individual data reductions for the amplitude and phase observations at the M_2 frequency. The actual amplitude and phase solutions were in terms of

amplitude times the sine and cosine of phase angle to avoid non-linearities.
The measurements corresponding to equation (5.4) are given in equations
(5.1), (5.2), and (5.3).

As previously indicated a value of k_2 and lag δ_2 must be assumed in order
to separate the ocean tide parameters. Table 12 gives the results obtained
when various values of k_2 and δ_2 are used. The solutions appear to be
reasonable, especially when one considers that no other satellite derived
M_2 tidal parameters have been published to date.

These estimates are systematically smaller than the results obtained from
numerical solution of Laplace tidal equations presented in table 4. The
quality of the results presented in table 12 can also be judged by how well
the prediction of the evolution of the mean lunar longitude with these
estimates matches the observed retardation of the lunar mean motion. This
comparison is given in chapter 6.

Table 10.--Amplitude and phase of inclination and node
perturbations due to the M_2 ocean tide on
GEOS-3 satellite

Source	Inclination Amplitude	Phase	Node Amplitude	Phase
Observed	0.040"	327°	0.027"	291°
Pekeris and Accad	0.051"	339°	0.030"	352°
Hendershott (Model 1)	0.061	317°	0.030"	286°
Hendershott (Model 2)	0.065"	276°	0.025"	244°
Bogdanov and Magarik	0.050"	328°	0.049	290°

Table 11. Mean Keplerian Elements (GEOS-3)

TIME (MJD)	A (METERS)	E	I (DEGREES)	NODE (DEGREES)	PERIGEE (DEGREES)	M (DEGREES)
42525.0	7219574.686	0.0004882	114.99295425	274.48228311	48.61929980	65.50701682
42527.0	7219576.837	0.0004961	114.99299087	279.93371283	47.00311446	173.27369786
42529.0	7219572.559	0.0005015	114.99397525	285.38499338	45.67152893	280.76031555
42531.0	7219576.155	0.0005086	114.99463393	290.83616337	43.98767899	28.59823389
42533.0	7219572.073	0.0005164	114.99562204	296.28746873	42.78774795	135.95201999
42535.0	7219574.238	0.0005218	114.99572488	301.73890939	41.13261257	243.76504650
42537.0	7219572.882	0.0005309	114.99561991	307.19041251	39.92174652	351.13032729
42539.0	7219571.436	0.0005362	114.99518986	312.64196159	38.47385703	98.73922242
42541.0	7219573.570	0.0005459	114.99444588	318.09342861	37.17156580	206.19825897
42543.0	7219569.254	0.0005521	114.99424180	323.54482439	36.01641110	313.51555560
42545.0	7219573.324	0.0005609	114.99391104	328.99608398	34.56906609	61.12367634
42547.0	7219569.026	0.0005689	114.99455323	334.44735744	33.56860079	168.28514994
42549.0	7219571.735	0.0005757	114.99499185	339.89866681	32.09866306	275.92247787
42551.0	7219570.089	0.0005857	114.99546126	345.34998605	31.16074386	23.01769886
42553.0	7219569.198	0.0005918	114.99527682	350.80133848	29.89744636	130.44706980
42555.0	7219571.028	0.0006025	114.99428755	356.25255261	28.85059745	237.65536090
42557.0	7219566.985	0.0006091	114.99347473	1.70360447	27.81741672	344.85485147
42559.0	7219570.864	0.0006186	114.99243843	7.15455516	26.55940009	92.27767135
42561.0	7219566.453	0.0006269	114.99241018	12.60545494	25.74746318	199.25501034
42563.0	7219569.202	0.0006349	114.99232789	18.05637785	24.49012208	306.68052504
42565.0	7219567.228	0.0006449	114.99270061	23.50728037	23.74031043	53.59442345
42567.0	7219566.574	0.0006518	114.99290526	28.95820738	22.59592000	160.90844077
42569.0	7219568.256	0.0006626	114.99266438	34.40898950	21.71228138	267.95642636
42571.0	7219564.737	0.0006697	114.99233141	39.85965449	20.78038771	15.05729127
42573.0	7219568.924	0.0006800	114.99111435	45.31006141	19.73728709	122.26723834
42575.0	7219564.693	0.0006883	114.99029696	50.76041229	19.04384251	229.12854989
42577.0	7219567.736	0.0006972	114.98933636	56.21082932	17.92948451	336.41355882
42581.0	7219565.131	0.0007151	114.98950686	67.11202591	16.18396703	190.49801969
42583.0	7219566.517	0.0007259	114.98968300	72.56250532	15.45389532	297.39468011
42585.0	7219562.952	0.0007330	114.98984708	78.01280314	14.60623573	44.41364991
42587.0	7219566.869	0.0007433	114.98912932	83.46281261	13.72199271	151.46680914
42589.0	7219562.235	0.0007514	114.98865931	88.91273152	13.06162287	258.29730159
42591.0	7219565.454	0.0007605	114.98766943	94.36260605	12.03005925	5.50110623
42593.0	7219562.910	0.0007699	114.98719724	99.81257147	11.44164026	112.25827146
42595.0	7219563.112	0.0007776	114.98685618	105.26268114	10.46170420	219.41243317
42597.0	7219564.318	0.0007827	114.98677245	110.71287301	9.83150441	326.21181984
42599.0	7219561.383	0.0007950	114.98725815	116.16315081	9.01790348	73.19989689
42601.0	7219565.207	0.0008051	114.98739531	121.61327745	8.22776041	180.16154119
42603.0	7219560.770	0.0008132	114.98784634	127.06322070	7.58006815	286.98216955
42605.0	7219563.903	0.0008226	114.98740563	132.51298673	6.65241007	34.08449447
42607.0	7219561.330	0.0008317	114.98700647	137.96281066	6.12958575	140.77918178
42609.0	7219561.501	0.0008403	114.98643920	143.41290433	5.21237410	247.87388073
42611.0	7219562.539	0.0008504	114.98615356	148.86319629	4.65992834	354.59900950
42613.0	7219559.279	0.0008583	114.98650998	154.31360724	3.84854139	101.58887292
42615.0	7219562.991	0.0008685	114.98672715	159.76391339	3.14780111	208.46499581
42617.0	7219558.319	0.0008763	114.98758191	165.21410779	2.52067087	315.26937053
42619.0	7219561.978	0.0008858	114.98785328	170.66417906	1.70262960	62.26603000
42621.0	7219559.025	0.0008945	114.98834552	176.11419628	1.21418191	168.93067016
42623.0	7219560.054	0.0009032	114.98837432	181.56432407	0.35299262	275.97359388
42625.0	7219560.722	0.0009130	114.98821867	187.01458102	359.85344985	22.65015953
42627.0	7219558.176	0.0009206	114.98816581	192.46518683	359.04945093	129.63712208
42629.0	7219561.490	0.0009303	114.98780705	197.91601624	358.41607347	236.45044199
42631.0	7219556.846	0.0009377	114.98830480	203.36706358	357.78380139	343.26546799
42633.0	7219560.353	0.0009471	114.98873567	208.81800609	357.02878804	90.20469770
42635.0	7219557.094	0.0009553	114.98980396	214.26865890	356.53459240	196.88105583
42637.0	7219557.929	0.0009641	114.99038357	219.71923190	355.70262633	303.90058197
42639.0	7219558.150	0.0009732	114.99056390	225.16986256	355.19230573	50.59392884
42641.0	7219558.384	0.0009812	114.99053621	230.62079550	354.60690277	157.56847399
42643.0	7219558.751	0.0009909	114.98995538	236.07185924	353.83292007	264.32830313
42645.0	7219554.174	0.0009990	114.98992265	241.52302369	353.19614093	11.15390553
42647.0	7219558.299	0.0010088	114.98956967	246.97410239	352.49101388	118.04889695
42649.0	7219554.930	0.0010173	114.98995088	252.42502948	351.96192163	224.76626156
42651.0	7219556.446	0.0010265	114.99025898	257.87584338	351.15693013	331.76445972
42653.0	7219556.207	0.0010356	114.99078111	263.32649908	350.66055450	78.44924646
42655.0	7219553.725	0.0010439	114.99133581	268.77721182	349.89978055	185.40417145
42657.0	7219556.661	0.0010537	114.99115735	274.22795007	349.37340121	292.12061960
42659.0	7219552.157	0.0010617	114.99087588	279.67890073	348.73838121	38.94899783
42661.0	7219556.043	0.0010714	114.98968717	285.12992038	348.06106137	145.82048696
42663.0	7219552.319	0.0010793	114.98917904	290.58082283	347.51165009	252.56324225
42665.0	7219553.789	0.0010883	114.98893281	296.03148204	346.76354688	359.50949362
42667.0	7219553.204	0.0010972	114.98929690	301.48185294	346.30913482	106.15706275
42669.0	7219551.080	0.0011057	114.98985332	306.93219026	345.58549716	213.07952648
42671.0	7219556.080	0.0011155	114.98985824	312.38248331	345.07322279	319.78620356
42673.0	7219549.903	0.0011235	114.98993469	317.83283716	344.42349082	66.63381446
42675.0	7219553.957	0.0011334	114.98910507	323.28311257	343.80368210	173.45141768
42677.0	7219550.087	0.0011415	114.98852222	328.73329415	343.28045017	280.17131915
42679.0	7219551.873	0.0011510	114.98756363	334.18335273	342.59049522	27.06229016
42681.0	7219551.069	0.0011601	114.98700641	339.63322200	342.14420355	133.70484370
42683.0	7219549.171	0.0011687	114.98695552	345.08308744	341.43451214	240.61689648
42685.0	7219551.912	0.0011788	114.98713105	350.53290898	340.92741391	347.32228335
42687.0	7219547.539	0.0011869	114.98803872	355.98283404	340.29028296	94.16155739
42689.0	7219551.499	0.0011969	114.98819341	1.43276068	339.71341705	200.93979288
42691.0	7219547.190	0.0012047	114.98814635	6.88261769	339.21306735	307.64073960
42693.0	7219549.216	0.0012143	114.98720014	12.33238028	338.54803708	54.51068993
42695.0	7219547.822	0.0012233	114.98647234	17.78204173	338.09357953	161.16644274
42697.0	7219546.464	0.0012321	114.98620239	23.23177229	337.40865017	268.05424759
42699.0	7219548.895	0.0012418	114.98617641	28.68150700	336.94194945	14.72975061
42701.0	7219544.721	0.0012495	114.98692377	34.13141758	336.33790408	121.54223468
42703.0	7219548.457	0.0012595	114.98730920	39.58138736	335.79430251	228.29349975
42705.0	7219544.156	0.0012670	114.98810342	45.03142703	335.29408762	335.00125508
42707.0	7219544.349	0.0012769	114.98819128	50.48143750	334.65691241	81.84970786
42709.0	7219544.896	0.0012855	114.98813255	55.93135820	334.22881743	188.48537352
42711.0	7219543.679	0.0012941	114.98773320	61.38128983	333.58350429	295.34494745
42713.0	7219545.967	0.0013038	114.98705096	66.83125635	333.15570082	41.98310880
42715.0	7219541.606	0.0013113	114.98703143	72.28147689	332.58274489	148.77170182
42717.0	7219545.447	0.0013222	114.98704298	77.73198597	332.07016231	255.49896367
42719.0	7219540.818	0.0013298	114.98802941	83.18268858	331.58652204	2.19746060
42721.0	7219543.386	0.0013397	114.98855830	88.63332574	330.99237426	109.00990879
42723.0	7219541.471	0.0013473	114.98895142	94.08371801	330.58333570	215.63368886

Table 12.—Ocean tide coefficients obtained with
various values of solid tide parameters

Fixed			Adjusted		
k_2	δ_2	$\overset{+}{C}_{22}$ (cm)	$\overset{+}{\varepsilon}_{22}$	$\overset{+}{C}_{42}$ (cm)	$\overset{+}{\varepsilon}_{42}$
0.30	0°	3.23	331°	.87	113°
.30	$\frac{1}{2}^{\circ}$	2.76	325°	.87	113°
.30	1°	2.32	318°	.87	113°
.31	0°	3.86	317°	.98	110°
.31	$\frac{1}{2}^{\circ}$	3.46	311°	.98	110°
.31	1°	3.11	303°	.98	110°

6. LUNAR ORBIT EVOLUTION

Analysis of ancient lunar eclipse and modern transit data has revealed a secular decay in the rate of change of the mean longitude of the Moon or equivalently a secular increase in the lunar orbital period. Any increase in the lunar period is reflected by an increase in the semi-major axis, since the period is equal to $\frac{1}{2\pi} \left[\frac{a^3_{Moon}}{G(m_{Earth} + m_{Moon})} \right]^{\frac{1}{2}}$. Since the total orbital energy is equal to $-G(m_{Earth} + m_{Moon})/2a_{Moon}$, the increase in a_{Moon} means that the Earth is transferring energy into the orbital motion of the Moon. This increase is accompanied by a decrease in the rotation rate of the Earth as well as energy loss due to the friction in the oceans and solid deformation. This orbital evolution of the Moon has been studied by Kaula (1969) and Lambeck (1975). Kaula investigated the effects of solid tides and Lambeck examined both solid and oceanic effects. The mean motion of any orbit is given by

$$N = \left[\frac{G(M + m_{Sat})}{a^3} \right]^{\frac{1}{2}}$$ (6.1)

where M is Earth mass. Any secular decay in the satellite's mean motion (or increase in orbital energy) can be found by differentiating (6.1) with respect to time

$$\dot{N} = -\frac{3}{2} \left(\frac{N}{a} \right) \dot{a}.$$ (6.2)

The next step is to substitute the appropriate solid or ocean potential into Lagrange planetary equations to obtain an expression for $\dot{a}$. From chapter 4.0, the potential for the lunar solid tide attraction is

$$\Delta U_{solid} = \frac{Gm^*}{a^*} \sum_{\ell m p q h j} k_\ell \left(\frac{a_e}{a^*}\right)^\ell \left(\frac{a_e}{a}\right)^{\ell+1} \frac{(\ell-m)!}{(\ell+m)!} \kappa_m \, F_{\ell m p}(i) \, G_{\ell p q}(e)$$

$$F_{\ell m h}(i^*) \, G_{\ell h j}(e^*) \, \cos(\upsilon^* - \upsilon + \varepsilon_{\ell m p q})$$

(6.3)

with $\quad \upsilon = (\ell-2p)\omega + (\ell-2p+q)M + m\Omega$

$\qquad \upsilon^* = (\ell-2h)\omega^* + (\ell-2h+j)M^* + m\Omega^*$

Remembering that $\dot{a} = \frac{2}{Na} \frac{\partial \Delta U}{\partial M}$, equation (6.3) can be differentiated and then substituted into (6.2). It is at this point that the satellite being studied is chosen to be the Moon. Thus, the Keplerian elements of the disturbing body (Moon) and the Keplerian elements of the satellite have the same value. That is, the Moon causes a deformation in the distribution of mass in the Earth which in turn affects the evolution of the lunar orbit. Now that the orbital elements of the satellite and the disturbing body are the same, the angular argument used in the $\dot{a}$ or $\dot{N}$ equation is

$$(2h-j-2p+q)M^* + (2h-2p)\omega^* + \varepsilon_{\ell m h j}.$$

Secular terms will occur when this angular argument contains only the constant $\varepsilon_{\ell m h j}$. Thus, for secular solid tidal decay, p must equal h, and q must equal j. da/dt is then given by

$$\dot{a}_{solid} = 2 \, B_{\ell m} [F_{\ell m h}(i^*) \, G_{\ell h j}(e^*)]^2 \, (\ell-2h+j) \, \sin \varepsilon_{\ell m h j}$$

(6.4)

$$B_{\ell m} = \frac{Gm^* k_\ell}{[G(M+m^*)a]^{\frac{1}{2}}} \left(\frac{a_e}{a}\right)^{2\ell+1} \frac{(\ell-m)!}{(\ell+m)!} \kappa_m .$$

Combining all possible combinations of lmpqhj, which would yield secular da/dt terms, the numerical representation for the second degree contribution

62

of solid tides to the orbital evolution of the moon is given as

$$\dot{N}_{solid} = -1040 \; k_2 \sin 2\delta_2 \; \text{arc seconds/century}^2$$

where δ_2 is the phase lag associated with the second degree harmonic.
Similarly the ocean tide potential

$$\Delta U_n = \frac{4\pi G a_e^2}{a} \sum_{\ell m p q} \frac{(1+k_\ell')}{2\ell+1} \left(\frac{a_e}{a}\right)^\ell \rho_w \; C_{n\ell m}^+ \; F_{\ell m p}(i) \; G_{\ell p q}(e) \begin{bmatrix} \sin \\ -\cos \end{bmatrix}_{\substack{\ell-m \; even \\ \ell-m \; odd}} \gamma_{\ell m p q}^+$$

$$\gamma_{\ell m p q}^+ = (\ell-2p)\omega + (\ell-2p+q)M + m(\Omega-\theta) + \bar{n}\cdot\bar{\beta} + \varepsilon_{n\ell m}^+ \qquad (6.5)$$

can be used to model the secular acceleration of the lunar mean motion
due to ocean tides. As with the solid tide, this is accomplished by
substituting equation (6.5) into Lagrange planetary equations and setting
the satellite elements equal to the lunar values. The equation of
interest is the da/dt equation

$$\dot{a}_{ocean} = 2B'_{n\ell m p q} \; (\ell-2p+q) \begin{bmatrix} \cos \\ \sin \end{bmatrix}_{\substack{\ell-m \; even \\ \ell-m \; odd}} \varepsilon_{\ell m}^+$$

$$\hspace{11cm} (6.6)$$

$$B'_{n\ell m p q} = \frac{3GM}{[G(M+m^*)a]^{\frac{1}{2}}} \; \frac{(1+k_\ell')}{2\ell+1} \; \frac{\rho_w}{\rho} \left(\frac{a_e}{a}\right)^\ell \; C_{n\ell m}^+ \; F_{\ell m p}(i)^* \; G_{\ell p q}(e^*)$$

where ρ is mean density of the Earth

The fourth-degree terms will experience a reduction of $(1/60)^2$ compared to
the second-degree terms. Thus, only the second degree terms need be
considered. By far the dominant tide is the lunar M_2 (solar terms will
be periodic). Lambeck obtains contributions to $\dot{N}_{moon}$ due to the N_2 and
O_1 ocean tide components of -4.4 arc seconds/century^2 which will be used

here. No other ocean tide components affect the lunar mean motion in a

secular manner. Values of lunar elements can be inserted into (6.6) with

ℓmpq = 2200 for the M_2 components to give

$$\dot{N}_{\text{ocean } M_2} = -8.21 \; C_{22}^+ \; \cos \; (\varepsilon_{22}^+) \; \frac{\text{arc seconds}}{\text{century}^2} \qquad (6.7)$$

The combined solid and ocean contributions yield the observation

equation

$$\dot{N}_{\text{total}} = [-1040 \; k_2 \; \sin \; (2\delta_2) \; -8.21 \; C_{22}^+ \; \cos(\varepsilon_{22}^+)$$

$$\qquad (6.8)$$

$$-4.4 \; (N_2+O_1)] \; \frac{\text{arc seconds}}{\text{century}^2}$$

Muller (1976) has performed an extensive analysis of ancient eclipses and

modern transit data (Morrison and Ward 1976) and obtains -27.2 ± 1.7 arc

seconds/century^2 for the lunar $\dot{N}$. The Morrison and Ward result is

-26.0 ± 2.0 arc seconds/century^2 from transits of Mercury. Lambeck evalu-

ated the lunar $\dot{N}_{\text{ocean } M_2}$ using the mean of three numerical tide models

and obtained -35 ± 4 arc seconds/century^2. At that time the accepted

value of $\dot{N}$ was in the vicinity of -35 to -40 arc seconds/century^2.

Lambeck's result seemed to agree with those recent values; he concluded

with the following:

"We conclude with confidence that if not all, at least a very major

part of the secular change in the Moon's mean longitude, is caused by

dissipation of tidal energy in the oceans, and we do not have to invoke

significant energy sinks in the Earth's mantle or core."

In light of the recent evaluations of lunar N, the value of -35 ± 4 arc seconds/century^2 would imply that the solid phase lag would be following rather than leading the Moon.

Using .30 and 0° as nominal values of k_2 and δ_2, respectively and the ocean tide values calculated in this study from 1967-92A and GEOS-3 perturbations, the value of $\dot{N}$ is $- 27.4 \pm 3$ arc seconds/century^2, a value which is in very good agreement with Muller, and Morrison and Ward. This result can be used also to argue that the effect of the solid tide must be small. Since the satellite-derived values of ocean tide parameters depend on what solid-tide values are used, table 13 gives the different solutions when the k_2 and lag angle are varied. Notice the consistency of $\dot{N}_{total}$ for various combinations of k_2 and δ_2. It is seen that even if the lag angle is changed by 0.5°, the resulting $\dot{N}$ changes by only 1 arc second/century^2. J. T. Kuo of Lamont-Doherty Geological Observatory (1977) analyzed data from a network of tidal gravimeters placed along a parallel of latitude across the United States and determined that the phase lag must be less than 1.0°--another result which is in harmony with the above quoted values.

Table 13.--Lunar $\dot{N}$ results with various values of k_2 and lag

κ_2	δ_2	C_{22}^+ (cm)	ε_{22}^+	$\dot{N}_{solid}$ arc sec/(100 yr)^2	$\dot{N}_{ocean}$ arc sec/(100 yr)^2	$\dot{N}_{total}$ arc sec/(100 yr)^2
0.30	0°	3.2	328°	0	-27.4	-27.4
.30	$\frac{1}{2}^\circ$	2.8	325	-5.4	-22.9	-28.4
.31	0°	3.9	317	0	-27.3	-27.3
.31	$\frac{1}{2}^\circ$	3.5	311	-5.6	-22.7	-28.3

The explanation for the larger influence of the ocean tide compared to the solid tide on the evolution of the mean longitude of the Moon can be obtained by examining the phase angles of the solid and ocean contributions. As discussed earlier, the solid bulge of the Earth, due to the attraction of the Moon, will lead the Moon by approximately 1.0° or less. The effective lead due to the oceans is found by subtracting ϵ_{22}^{+} from 90°, so that the $\dot{N}_{total}$ given in equation (6.8) is expressed in terms of 2 sine functions. Since the angular argument is proportional to frequency (Darwinian assumption discussed in chapter 4) the lead due to oceans is

$$\delta_{22}^{oceans} = \frac{90^{\circ}-(-20^{\circ})}{2} = 55^{\circ}$$

Also, the degree and order harmonic (2,2) physically represents an equatorial ellipticity or the equivalent ocean tide bulge. Thus, even though the direct attraction of the ocean tide is much smaller than the solid tide, the resulting torque of the oceans generated by the large 55° lead actually dominates the behavior of the small secular decay in the mean motion of the Moon.

APPENDIX I.—SOLID TIDE POTENTIAL IN TERMS OF DISTURBING

BODY'S ECLIPTIC ELEMENTS

Transforming from the equatorial coordinate system to the ecliptic can
be accomplished in two ways. The first would be the obvious technique of
converting the three coordinate dependent variables node, perigee, and
inclination of the body into ecliptic elements. The second technique,
and the one that is used here, is to rotate the surface harmonic terms
due to the disturbing body from the equatorial to the ecliptic system.
This method is not only direct, but also yields the potential in a form
that allows easy analysis of the fundamental frequencies. Returning to
Kaula (1962), one finds that

$$\Delta U(r) = \frac{Gm^*}{r^*} \sum_{n=2}^{\infty} k_n \left(\frac{a_e}{r^*}\right)^n \left(\frac{a_e}{r}\right)^{n+1} P_n(\cos S) \quad ,$$

where starred quantities refer to the disturbing body , unstarred
quantities refer to the satellite, and S is the angle from disturbing body
to center of the Earth to the satellite, can be expressed as

$$\Delta U_n = \frac{Gm^*}{r^*} \left(\frac{a_e}{r^*}\right)^n \left(\frac{a_e}{r}\right)^{n+1} k_n \left[P_n(\sin \delta) \, P_n(\sin \delta^*) + 2 \sum_{m=1}^{n} \frac{(n-m)!}{(n+m)!} \, P_{nm}(\sin \delta) \right.$$

$$\left. P_{nm}(\sin \delta^*) \, (\cos m\alpha \cos m\alpha^* + \sin m\alpha \sin m\alpha^*) \right]$$

(I.1)

where P_{nm} is the associated Legendre function, δ and δ^* are declination
of satellite and body, respectively; and α and α^* are right ascension of
satellite and body, respectively.

Since both (α,δ) and (α^*,δ^*) are in an Earth-equatorial system, it is
necessary only to transform the starred terms to the ecliptic. This
is a rather simple transformation, since both the ecliptic and equatorial

67

systems have the x-axis in common. Let ε be the angle of rotation about the x-axis from the equatorial plane to the ecliptic system (obliquity of the ecliptic). Then any vector $\overline{P}_{ec}$ whose components are known in the ecliptic system can be expressed in the equatorial system by the matrix relation

$$\overline{P}_e = A \, \overline{P}_{ec}$$

where

$$A = \begin{bmatrix} 1 & 0 & 0 \\ 0 & \cos \varepsilon & -\sin \varepsilon \\ 0 & \sin \varepsilon & \cos \varepsilon \end{bmatrix}$$

Let

$$Y_{nm}(\phi,\lambda) = P_{nm}(\sin\phi)\exp(im\lambda) \tag{I.2}$$

be a surface harmonic of degree n and order m. Alternatively (I.2) can be written as

$$Y_{nm}(\phi,\lambda) = P_{nm}(\sin\phi)[\cos m\lambda + i \sin m\lambda]$$

$$= Y_{nm}^R(\phi,\lambda) + Y_{nm}^I(\phi,\lambda) \, i \tag{I.3}$$

where R and I stand for real and imaginary components, respectively. (I.1) can now be rewritten as

$$\Delta U_n = \frac{Gm^*}{r^*} \left(\frac{a_e}{r^*}\right)^n \left(\frac{a_e}{r}\right)^{n+1} k_n \left[\sum_{m=0}^{n} \kappa_m \left\{ Y^R(\alpha,\delta) \, Y^R(\alpha^*,\delta^*) + Y^I(\alpha,\delta) \, Y^I(\alpha^*,\delta^*) \right\} \right] . \tag{I.4}$$

Courant and Hilbert (1953) have provided the necessary formulas for expressing any surface harmonic in a desired coordinate system as the linear combination of surface harmonics in another system

68

$$Y_{nm}(\phi,\lambda) = \sum_{r=-n}^{n} \frac{(n-r)!}{(n-m)!} S_{2n}^{(m,r)}(\rho,\sigma,\tau) \; Y_{nr}(\phi',\lambda')$$

(I.5)

$$S_{2n}^{(m,r)}(\rho,\sigma,\tau) = \frac{1}{(n+r)!} \exp[-i(m+r)\rho] \exp[-i(r-m)\sigma] (\cos \tau)^{m+r}(\sin \tau)^{r-m} \cdot$$

$$F_{2n}^{(m,r)}(\cos^2\tau)$$

$$F_{2n}^{(m,r)}(x) = \frac{d^{n+r}}{dx^{n+r}} x^{n-m} (x-1)^{n+m}$$

where ρ, σ, τ depend on the rotation. For the particular rotation at hand, the proper set of arguments are $\rho=0$, $\sigma=\pi/2$, $\tau=\epsilon/2$. (I.5) can now be rewritten so that any linear factor on the right is expressed as a product of a scale factor and rotation factor

$$Y_{n\ell}(\phi,\lambda) = \sum_{r=-n}^{n} \psi_{n\ell r}(\epsilon/2) \exp[-i(r-\ell)\pi/2] \; Y_{nr}(\phi',\lambda')$$

(I.6)

The $\psi_{n\ell r}$ values are rather easy to compute using equation (I.5). As one might expect, the largest contribution occurs when $r = \ell$. For example, the important $Y_{22}(\phi,\lambda)$ term would be given as

$$P_{22}(\sin\phi) \exp(i2\lambda) = .17\times10^{-2} \qquad P_{22}(\sin\phi') \exp(-2i\lambda')$$

$$+.33\times10^{-2} \exp(3\pi i/2) \; P_{21}(\sin\phi') \exp(-i\lambda')$$

$$-.47 \qquad P_{20}(\sin\phi')$$

$$-.76 \qquad \exp(\pi i/2) \; P_{21}(\sin\phi') \exp(i\lambda')$$

$$+.92 \qquad P_{22}(\sin\phi') \exp(2i\lambda')$$

where advantage has been taken of the relation

$$P_{n,-\ell}(x) = (-1)^{\ell}\, \frac{(n-\ell)!}{(n+\ell)!}\, P_{n,\ell}(x) \ .$$

Substituting (I.6) into (I.1) and carrying on in the same fashion as Kaula did yields results similar to his,

$$\Delta U = Gm^* \sum_{n=2}^{\infty} \sum_{m=0}^{n} \sum_{p=0}^{n} \sum_{q=-\infty}^{\infty} \sum_{k=-n}^{n} \sum_{h=0}^{|k|} \sum_{j=-\infty}^{\infty} k_n \left(\frac{a_e}{a}\right)^{n+1} \psi_{nmk}^* \frac{a_e^n}{a^{*n+1}} \kappa_m$$

$$\frac{(n-m)!}{(n+m)!}\, F_{nmp}(i)\, F_{n|k|h}(i^*)\, G_{npq}(e)\, G_{nhj}(e^*) \begin{bmatrix} \cos \\ (-1)^{n-k}\sin \end{bmatrix}^{\substack{m-k \ \text{even} \\ \rho \\ m-k \ \text{odd}}} \tag{I.7}$$

$$\rho = (n-2p)\omega + (n-2p+q)M + m\Omega - (n-2h+j)M^* - (n-2h)\omega^* - |k|\Omega^* + \mathrm{sgn}(k)(k-m)\pi/2 \ .$$

$$\psi_{nmk}^* = \begin{cases} \psi_{nmk}\ (-1)^k\, \dfrac{(n-|k|)!}{(n+|k|)!} & \text{if } k < 0 \\[2ex] \psi_{nmk} & \text{if } k \geq 0 \end{cases}$$

and now the starred variables refer to the ecliptic elements of the disturbing body.

70

REFERENCES

Bogdanov, K. T., and Magarik, V. A., 1967: Numerical solutions for the world's semi-diurnal (M_2 and S_2) tides. *Dokl. Akad. Nauk SSSR*, 172, 1315-1317.

Brown, E. W., and Shook, A. S., 1964: *Planetary Theory*. Dover Publications, Inc., New York, 302 pp.

Clancy, E. P., 1968: *The Tides: Pulse of the Earth*. Doubleday, New York, N. Y.

Clemence, G. M., and Brouwer, D., 1961: *Methods of Celestial Mechanics*. Academic Press, New York, 598 pp.

Courant, R., and Hilbert, D., 1953: *Methods of Mathematical Physics*. Interscience Publishers, New York, N. Y., Vol. 1, 543-545.

Darwin, G. H., 1962: *The Tides and Kindred Phenomena in the Solar System*. W. H. Freeman and Company, San Francisco, Calif., 378 pp. (originally published 1898).

Doodson, A. T., 1921: The harmonic development of tide generating potential. *Proceedings of the Royal Society London*, Serial A, No. 100, 305-329.

Douglas, B. C., Klosko, S., Marsh, J. G., and Williamson, R. G., 1972: Tidal perturbations on the orbits of GEOS 1 and GEOS 2. NASA Document X-553-72-475, Goddard Space Flight Center, Greenbelt, Md.

Douglas, B. C., Klosko, S., Marsh, J. G., and Williamson, R. G., 1974: Tidal parameters from the variation of inclination of GEOS-1 and GEOS-2. *Celestial Mechanics*, 10, 165-178.

Farrell, W. E., 1972: Deformation of the earth by surface loads. *Review Geophysics Space Physics*, 10, 761-797.

Hendershott, M., and Munk, W., 1970: Tides, *Annual Review of Fluid Mechanics*, 21, 205-224.

Hendershott, M. C., 1972: The effects of solid earth deformations on global ocean tides, *Geophysical Journal Royal Astronomical Society*, 29, 389-402.

Jeffreys, H., 1970: *The Earth*. Cambridge University Press, Cambridge, England, 5th edition, 525 pp.

Kaula, W. M., 1961: Development of the lunar and solar disturbing functions for a close satellite. *Astronomical Journal*, 67, 300-303.

Kaula, W. M., 1966: *Introduction to Satellite Geodesy*. Blaisdell, Waltham, Mass., 124 pp.

Kaula, W. M., 1968: An Introduction to Planetary Physics. John Wiley, New York, N. Y., 490 pp.

Kaula, W. M., 1969: Tidal friction with latitude dependent amplitude and phase angle. Astronomical Journal, 74, 1108-1114.

Kozai, Y., 1965: Effects of the tidal deformation of the earth on close earth satellites. Publication of Astronomical Society Japan, 17, 395-402.

Kozai, Y., Love's number of the earth derived from satellite observations, Publication of Astronomical Society Japan, 20, 24-26.

Kuo, J. T. (Lamont-Doherty Geological Observatory, Columbia University, Palisades, New York), 1977 (personal communication).

Lambeck, K. 1975: Effects of tidal dissipation in the oceans on the moon's orbit and the earth's rotation. Journal of Geophysical Research, 80, 2917-2925.

Lambeck, K., Cazenane, A., and Balmino, G., 1974: Solid earth and ocean tides estimated from satellite orbit analyses. Reviews of Geophysics and Space Physics, 12, 421-434.

Lerch, F. J., Wagner, C. A., Richardson, J. A., and Brownd, J. E., 1974: Goddard Earth Models (5 and 6), NASA Document X-921-74-145. National Aeronautics and Space Administration, Goddard Space Flight Center, Greenbelt, Md.

MacRobert, T. M., 1967: Spherical Harmonics: Pergamon Press, Oxford, England, 349 pp.

Menzel, D. H., 1961: Mathematical Physics. Dover Publications, Inc., New York, N. Y., 412 pp.

Morrison, L. V., and Ward, C. G., 1975: An analysis of the transits of Mercury 1677-1973. Monthly Notices of Royal Astronomical Society, London, 173, 183-206.

Muller, P. M., 1976: Determination of the Cosmological Rate of Change of G and the Tidal Accelerations of Earth and Moon from Ancient and Modern Astronomical Data, JPL SP 43-36, Jet Propulsion Laboratory, Pasadena, Calif.

Munk, W. H., and MacDonald, G. J. F., 1960: The Rotation of the Earth. Cambridge University Press, London, England, 323 pp.

NASA (U. S. National Aeronautics and Space Administration), 1974: GEOS-C Mission Plan, NASA Wallops Flight Center, Wallops Island, Va.

Newton, R. R., 1965: An observation of the satellite perturbation produced by the solar tide, Journal of Geophysical Research, 70, 5983-5989.

Newton, R. R., 1968: A satellite determination of tidal parameters and earth deceleration. Geophysical Journal Royal Astronomical Society, 14, 505-539.

Pekeris, C. L., and Accad, Y., 1969: Solutions of Laplace's equations for M_2 tide in the world oceans. Philosophical Transactions of the Royal Society, London, Serial A, Vol. 265, 413-436.

Wagner, C. A., and Douglas, B. C., 1970: Resonant satellite geodesy by high speed analysis of mean Kepler elements, in Dynamics of Satellites (1969), Morando, B. (editor). Springer-Verlag, Berlin, Germany, 130-137.

Wagner, C. A., Lerch, F. J., Brownd, J. E., and Richardson, J. A., 1976: Improvement in the geopotential derived from satellite and surface data (GEM 7 and 8), NASA, Goddard Space Flight Center, Greenbelt, Md., Document X 921-76-20.

Williamson, R. G., and Mullins, N. E., 1973: ROAD USERS GUIDE, Wolf Research and Development Corporation, Riverdale, Md. Report on NASA contract NAS 5-11932-37.

NOAA Technical Reports National Ocean Survey,
National Geodetic Survey Subseries

NOS 65 NGS 1   The statistics of residuals and the detection of
                outliers. Allen J. Pope, May 1976, 133 pp.

NOS 66 NGS 2   Effect of Geoceiver observations upon the
                classical triangulation network. Robert E. Moose
                and Soren W. Henriksen, June 1976, 65 pp.

NOS 67 NGS 3   Algorithms for computing the geopotential using
                a simple-layer density model. Foster Morrison,
                March 1977, 41 pp.

NOS 68 NGS 4   Test results of first-order class III leveling.
                Charles T. Whalen and Emery Balazs, November 1976,
                30 pp.

NOS 70 NGS 5   Selenocentric geodetic reference system.
                Frederick J. Doyle, Atef A. Elassal, and
                James R. Lucas, February 1977, 53 pp.

NOAA Technical Memorandums National Ocean Survey,
National Geodetic Survey Subseries

NOS NGS 1   Use of climatological and meteorological data in the
             planning and execution of National Geodetic Survey
             field operations. Robert J. Leffler, December 1975,
             30 pp.

NOS NGS 2   Final report on responses to geodetic data question-
             naire. John F. Spencer, Jr., March 1976, 39 pp.

NOS NGS 3   Adjustment of geodetic field data using a sequential
             method. Marvin C. Whiting and Allen J. Pope,
             March 1976, 11 pp.

NOS NGS-4   Reducing the profile of sparse symmetric matrices.
             Richard A. Snay, June 1976, 24 pp.

NOS NGS-5   National Geodetic Survey data: Availability, expla-
             nation, and application. Joseph F. Dracup, June
             1976, 39 pp.

NOS NGS-6   Determination of North American Datum 1983 coordin-
             ates of map corners. T. Vincenty, October 1976, 8 pp.